Externally Controlled Atom Transfer Radical Polymerization

Journal:	*Chemical Society Reviews*
Manuscript ID	CS-REV-04-2018-000259.R1
Article Type:	Review Article
Date Submitted by the Author:	09-May-2018
Complete List of Authors:	Matyjaszewski, Krzysztof; Carnegie Mellon University, Department of Chemistry Fantin, Marco; Carnegie Mellon University, Department of Chemistry Pan, Xiangcheng ; Fudan University Yuan, Fang ; Fudan University

Externally Controlled Atom Transfer Radical Polymerization

Xiangcheng Pan,[a,*] Marco Fantin,[b] Fang Yuan,[a] Krzysztof Matyjaszewski[b,*]

a. State Key Laboratory of Molecular Engineering of Polymers, Department of Macromolecular Science, Fudan University, Shanghai 200433, China.

b. Department of Chemistry, Carnegie Mellon University, Pittsburgh, PA 15213, United States

XP: panxc@fudan.edu.cn; KM: km3b@andrew.cmu.edu

I. Introduction

The 1956 landmark work on anionic living polymerization instigated the development of other advanced ionic and coordination controlled/living polymerizations procedures.[1, 2] In an ideal living polymerization system, all polymer chains grow at the same rate without irreversible transfer or termination reactions. Since radical-radical termination is unavoidable and diffusion-controlled, a pure living process is impossible to achieve in radical polymerization.[3-5] The concept of creating a dynamic equilibrium between active and dormant species was therefore introduced to radical polymerization, which offered well-defined polymers with narrow molecular weight distribution and preserved chain-end functionality, but with some degree of termination (or transfer) reactions. These systems are often described as controlled radical polymerizations (CRPs), controlled/living, “living”, or, as suggested by IUPAC, reversible-deactivation radical polymerizations (RDRPs).[6, 7]

The most frequently used CRP systems are stable free-radical polymerization (SFRP, including nitroxide mediated polymerization and organometallic radical polymerization),[8-11] atom transfer radical polymerization (ATRP),[12-22] and degenerative chain-transfer (DT) polymerization.[23-26] Control in all these systems is established by formation of a dynamic equilibrium between the predominant dormant species and a low concentration of propagating radicals. ATRP offers a simple experimental setup that is applicable to a broad range of monomers, utilizing ligands, catalysts, solvents, and commercially available alkyl halides initiators with various structures, which can be attached to surfaces or biological molecules.

In an ATRP equilibrium, alkyl halides initiators (RX, X = Br or Cl) or macromolecular species (P_m-X) are the dormant species that react with a transition metal complex in a lower oxidation state to provide initiating ($R^{\bullet}$) or growing oligo/polymeric radicals ($P_m^{\bullet}$) and transition metal complexes in higher oxidation state, which act as deactivators. Before deactivation of the propagating radicals by the transition metal in the higher oxidation state, these intermittently formed radicals initiate or propagate the polymerization. Initially, relative high concentrations (ca. 1000 to 10,000 ppm) of low activity copper catalysts were used to overcome the irreversible radical termination and formation of the required concentration of deactivator, according to the persistent radical effect.[27-29]

Significant advances have been made that allow use of parts per million (ppm) catalyst loadings in ATRP reactions through continuous regeneration of activators (complexes in the lower oxidation state) from deactivators (complexes in the higher oxidation state). To reflect the reactivation mechanisms, these procedures have been termed as activator regeneration by electron transfer (ARGET) ATRP with various reducing agents,[30] initiators for continuous activator regeneration (ICAR) ATRP with conventional radical initiators,[31] or supplemental activator and reducing agent (SARA) ATRP with zerovalent metals, [32-40] which was also termed single electron transfer living radical polymerization (SET-LRP).[41-43] Several procedures that allow spatial and temporal regulation of controlled polymerizations by external stimuli such as light, ultrasound, and electric current have been recently developed.[44, 45] These nonchemical methods include electrochemically mediated polymerization (*e*ATRP) [46-49], photochemically mediated polymerization (photoATRP), [50-52] and mechanochemically mediated procedures (mechanoATRP).[53-56]

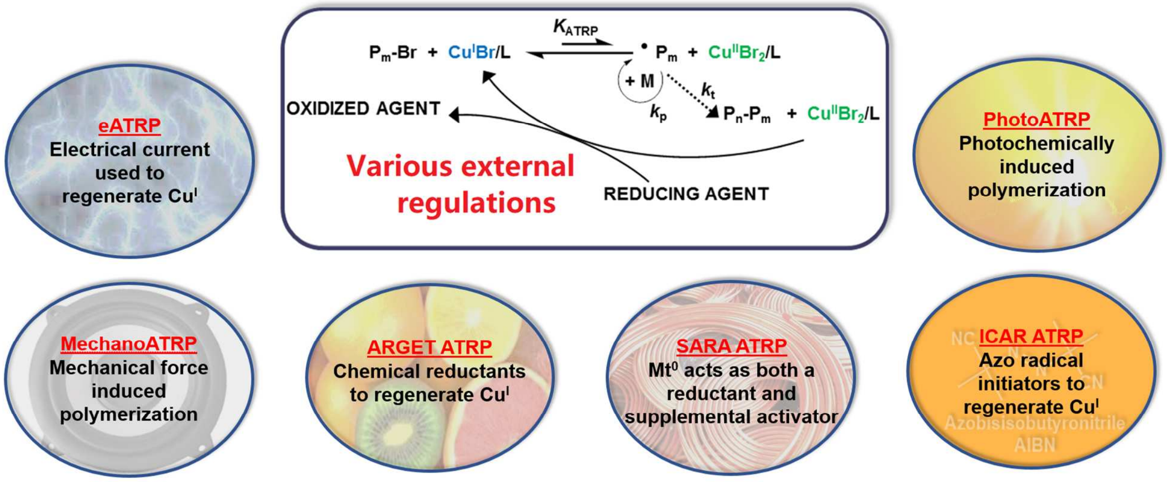

Figure 1. External control of various ATRP techniques.

Many of these external stimuli have been applied to ATRP techniques as shown in **Figure 1**. *e*ATRP, photoATRP, and mechanoATRP are externally controlled by electrical current, light, and mechanical forces, respectively. Conversely, ARGET and SARA ATRP could be considered as chemically controlled processes by redox modulation using chemical reducing agents which can be fed to the reaction (in SARA ATRP, the chemical reducing agents also behave as supplemental activators and, for example, can be periodically removed from the reaction mixture). ICAR ATRP is a thermally regulated process through decomposition of radical initiator and can be controlled by changing the temperature and also the feeding rate of the initiators.

The aim of this review is to highlight the use of external regulation in ATRP and to summarize the present state-of-the-art and future perspectives, focusing on mechanistic aspects, synthetic procedures, preparation of polymers with complex architecture and functional materials, and their applications. Special emphasis will be given to rapidly developing *e*ATRP, photoATRP, and recently reported mechanoATRP.

II. *e*ATRP

2.1 Mechanism

In *e*ATRP, electrodes with relatively large surface area (ca. 5 cm^2) were used as the electron source for the bulk electrolysis of $X\text{-}Cu^{II}L^+$, which then generated Cu^IL^+ and triggered controlled polymerization.[46, 49] *e*ATRP was generally carried out in a three-electrode setup, which was described in detail in references.[49, 57] In *e*ATRP, electrons were directly used as 'reducing agents', thus avoiding the formation of any byproducts from activator regeneration. Polymer contamination was minimized when separating the anodic compartment from the cathodic one, where polymerization occurred. Most importantly, polymerization was strictly controlled by the applied electrochemical parameters, such as potential and current, which were selected based on the electrochemical properties of the catalyst.

The catalyst was typically screened by cyclic voltammetry (CV). An example for the *e*ATRP of *n*-butyl acrylate (BA) catalyzed by Cu/tris(2-pyridylmethyl)amine (TPMA) is presented in **Figure 2A**. The Cu^{II}/L catalyst complex typically had a well-defined and reversible redox wave, from which the half-wave potential was calculated as $E_{1/2} = (E_{pc} + E_{pa})/2$, where E_{pc} and E_{pa} were the cathodic and anodic peak potentials. Addition of a RX initiator modified the voltammetric pattern, increasing the cathodic peak current I_{pc} and decreasing the anodic one I_{pa}. This was due to the occurrence of the *e*ATRP electrocatalysis as presented in **Scheme 1**. First, X-$Cu^{II}L^+$ was reduced to X-$Cu^{I}L$, which partially dissociated to X^- + Cu^IL^+. The latter was involved in the ATRP equilibrium, resulting in the generation of radicals and reformation of X-Cu^{II}/L^+, which closed the catalytic cycle. Radicals propagated with monomer and eventually terminated.

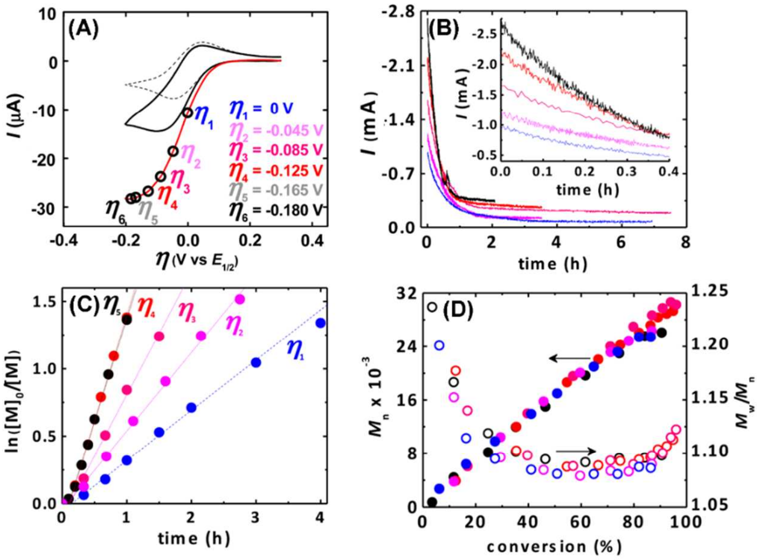

Figure 2. *e*ATRP as a function of E_{app} at overpotential (η) ranging from 0 to −0.165 V. (A) CV of 1 mM Br−Cu^{II}/$TPMA^+$ in 56% (v/v) BA/DMF + 0.2 M *n*-Bu_4NClO_4 recorded at a scan rate (v) of 50 mV/s in the absence (dashed black) and presence (solid black) of 13 mM EBiB. Linear sweep voltammetry (solid red) using an identical formulation to those in CV containing EBiB under convection. Black circles correspond to applied potential values (E_{app}), expressed as η values, used in *e*ATRP experiments. (B) Current versus time, (C) first-order plot of monomer conversion versus time, and (D) M_n and M_w/M_n versus conversion. Reaction conditions: $[BA]_0/[EBiB]_0/[Br{-}Cu^{II}TPMA^+]_0$ = 300/1/0.09, $[n\text{-}Bu_4NClO_4]_0$ = 0.2 M, $[BA]_0$ = 3.9 M in DMF, T = 44 °C, V_{tot} = 23 mL, and stirring rate = 875 rpm. For clarity η_6 = −0.180 V was omitted from (B), (C), and (D). Reproduced from ref. [58] with permission from the American Chemical Society, copyright 2013.

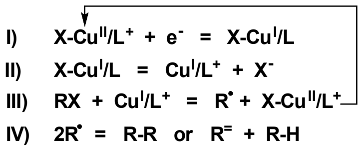

I) $X\text{-}Cu^{II}/L^+ + e^- = X\text{-}Cu^I/L$

II) $X\text{-}Cu^I/L = Cu^I/L^+ + X^-$

III) $RX + Cu^I/L^+ = R^\bullet + X\text{-}Cu^{II}/L^+$

IV) $2R^\bullet = R\text{-}R$ or $R^= + R\text{-}H$

Scheme 1. Electrocatalytic mechanism in *e*ATRP.

In potentiostatic *e*ATRP, polymerization was started by applying a fixed potential (E_{app}) close to or more negative than $E_{1/2}$ (**Figure 2A**). Application of E_{app} under stirring generated a cathodic current due to reduction of Cu^{II} species (**Figure 2B**). Polymerization rate depended on the applied "overpotential" $\eta = E_{\text{app}} - E_{1/2}$. More negative η caused higher cathodic currents, which translated to faster polymerization rates (**Figure 2C**). Polymerization rate changed with η due to modulation of the $\text{Cu}^{\text{II}}/\text{Cu}^{\text{I}}$ ratio on the surface of the electrode as expressed by the following relationship:[59, 60]

$$\eta = \frac{RT}{F}\ln\frac{[\text{X}-\text{Cu}^{\text{II}}\text{L}^{+}]}{[\text{X}-\text{Cu}^{\text{I}}\text{L}]} \qquad \textbf{(Equation 1)}$$

where R is the gas constant and F is the Faraday constant. The rate increase reached saturation at η_4 value, due to mass transfer limitation. The total consumed charge was used to estimate the extent of radical-radical termination during an *e*ATRP. In fact, each termination event (i.e. one consumed radical) caused the accumulation of one molecule of Cu^{II} complex and its successive one-electron reduction to Cu^{I}, with the consumption of one elementary charge.[61-63] Therefore, *e*ATRP not only allows for an external regulation of polymerization, but also for *in situ* monitoring of the reaction though information such as consumed charge and cyclic voltammetry of complexes.

The overpotential, η, also modulated dispersity; more negative η values established a lower $\text{Cu}^{\text{II}}/\text{Cu}^{\text{I}}$ ratio, which caused slightly higher dispersity due to a slower rate of deactivation. This effect was quite small for the polymerization using highly effective Cu/TPMA in DMF (**Figure 2D**), but stronger modulation of $Đ$ with overpotential was reported in water,[64] in ionic liquids,[65] or in DMF with Cu/*N*,*N*,*N*',*N*'',*N*''-pentamethyldiethylenetriamine (PMDETA) ligand.[58] Similar properties were obtained when using the $\text{Fe}^{\text{III}}/\text{Fe}^{\text{II}}$ redox couple with phosphine ligands, but with inferior polymerization control.[66-68]

Temporal polymerization control was obtained by switching η between $\eta < 0$ and $\eta >> 0$, **Figure 3A**. Application of a positive overpotential caused rapid oxidation of $\text{Cu}^{\text{I}}/\text{L}$ to $\text{Cu}^{\text{II}}/\text{L}$ deactivators, which quickly halted the polymerization. Complete reinitiation resulted after switching again to negative η, confirming preservation of dormant ATRP chain ends. *e*ATRP allowed for very accurate temporal control. Without application of an oxidation potential, polymerization slowly decelerated due to radical termination and not due to direct oxidation of the catalyst.

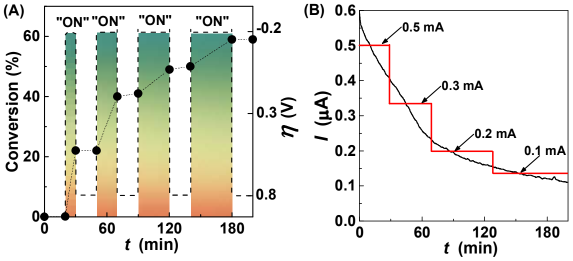

Figure 3. (A) Variation of conversion (black circles) and applied potential (dashed lines) with time during *e*ATRP of methacrylic acid; no potential was applied during the first 20 min. C_M:C_{RX}:$\boldsymbol{C}_{\mathbf{CuCl_2}}$:$C_{TPMA}$: C_{NaCl} = 200:1:0.1:0.4:29, T = 25 °C. Reproduced from reference [62] with permission from the American Chemical Society, copyright 2016. (B) Splitting of a chronoamperometry recorded during potentiostatic *e*ATRP into several galvanostatic steps. Reproduced from reference [69] with permission from Wiley, copyright 2016.

Catalytic halogen exchange. Exchange of chain-end halogen from C-Br to C-Cl was required when building a block copolymer where the second block was more active (i.e. had higher K_{ATRP}) than the first block.[70] Electrochemical regeneration of a small amount of Cu^I/L (10 mol % with respect to P_n-Br) allowed complete conversion of the chain end of the macroinitiator from C-Br to C-Cl, in the presence of an amount of Et_4NCl equimolar to the initiator.[65] Without regeneration of Cu^{II} through the external electrochemical control, the halogen exchange (HE) required high concentrations of catalyst, i.e. adding an amount of Cu^ICl/L equal to, or higher than, the amount of P_n-Br chain ends,[71-81] which ensured complete conversion of P_n-Br to P_n-Cl.

The mechanism of catalytic halogen exchange (cHE) under electrochemical control is illustrated in **Figure 4A** for the chain extension of poly(methyl acrylate)-Br (PMA-Br) with acrylonitrile (AN). Once PMA-Br was activated (step I), the generated radical quickly added one or more molecules of acrylonitrile, which was present in a large excess in the polymerization mixture (step II). In presence of excess Cl^-, most of the deactivator complex was converted to Cl-$Cu^{II}L^+$, because of the higher affinity of Cu^{II} for Cl^- than Br^- (step III). [64, 82, 83] Then, the polyacrylonitrile (PAN) chain end was preferentially deactivated by Cl-Cu^{II}TPMA$^+$, regenerating the active Cu^IL^+ and a Cl-capped dormant chain (step IV). cHE had good reinitiation of PMA-Br (**Figure 4B**), whereas poor reinitiation was observed in the absence of excess Et_4NCl, which prevented complete halogen exchange (**Figure 4C**).

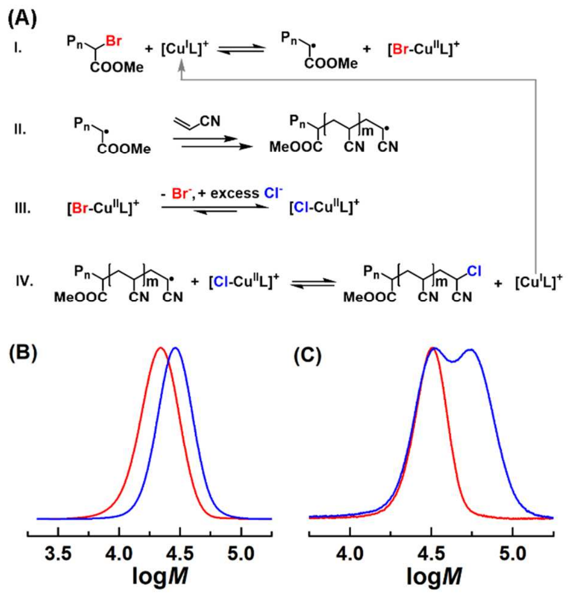

Figure 4. (A) Mechanism of cHE. (B-C) *e*ATRP of 50% (v/v) AN in [BMIm][OTf] + PMA-Br macroinitiator performed at $E_{\mathrm{app}} = E_{1/2}$ - 0.06 V; $C_{\mathrm{AN}}:C_{\mathrm{PMA\text{-}Br}}:C_{\mathrm{CuBr_2}}:C_{\mathrm{TPMA}}:C_{\mathrm{Et_4NCl}}$ = 740:1:0.1:0.1:x; (B) x = 1.2; (C) x = 0. $C_{\mathrm{CuBr_2}} = 10^{-3}$ M. GPC traces recorded before (—) and after (—) chain extension. Reproduced from reference [65] with permission from the Royal Society of Chemistry, copyright 2018.

Simplification of the eATRP setup. Several modifications and simplifications of the *e*ATRP setup from the original three-electrode setup have been developed. The traditionally used platinum working electrode was substituted with less expensive and more available metals or carbon based materials (e.g. stainless steel, NiCr alloys, glassy carbon).[69, 84]

In typical *e*ATRP setups, the counter electrode was separated from the polymerization media by using a two-compartment reactor. The separator could be removed by using a sacrificial Al anode.[47, 85-91] In this case, excess ligand should be used to complex the released Al^{3+}.[84]

*e*ATRP in water or in organic solvents generally required a supporting electrolyte to enhance conductivity. Ionic liquids, however, had sufficient conductivity to carry out an *e*ATRP without any supporting electrolyte.[65, 82] The ionic liquid/catalyst mixture was recycled several times after simple extraction of the polymer in toluene.

Galvanostatic *e*ATRP required a simpler two-electrode setup (without reference electrode), instead of the traditional three-electrode setup. The current program was composed of multiple current steps set to mimic the current decay of a potentiostatic *e*ATRP (**Figure 3B**). *e*ATRP with two-electrode setup could be carried out with a simpler current generator instead of a potentiostat.[49]

Copper removal. Application of $\eta << 0$ caused the reduction of Cu^{I}/L^{+} to $Cu^{0} + L$. The generated Cu^{0} deposited on the working electrode, allowing for easy purification of the reaction mixture.[58, 92] Cu was removed also from a miniemulsion system, enhancing the stability of the latex.[93]

2.2 Miniemulsion

Dispersed media are challenging for *e*ATRP because the electrode is in contact with the continuous aqueous phase, while the reaction occurs in the dispersed hydrophobic droplets. Two approaches were developed to promote electrochemical communication between the electrode and the polymerizing droplets.

Dual catalysis. A dual-catalyst system was developed to deliver the electrochemical stimulus from the aqueous phase to the droplets. The system was composed of one hydrophilic and one hydrophobic catalyst.[94] Well-defined poly(*n*-butyl acrylate) (PBA) homopolymers and block copolymers were obtained with a water soluble Cu/*N*,*N*-bis(2-pyridylmethyl)-2-hydroxyethylamine (BPMEA) complex (Cu/L_{aq}) in combination with a hydrophobic Cu/bis[2-(4-methoxy-3,5-dimethyl)-pyridylmethyl]octadecylamine (BPMODA∗) (Cu/L_{org}), soluble in the dispersed organic phase. The mechanism of this “dual catalyst” system is presented in **Scheme 2A**. $X\text{-}Cu^{II}L_{aq}$ was reduced at the working electrode. Then, the more hydrophobic cuprous catalyst migrated to the organic phase, where it could reduce the organic phase catalyst that effectively controlled the polymerization.

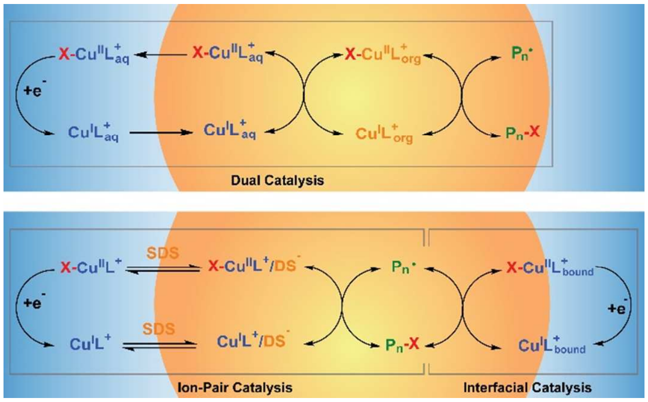

Scheme 2. Mechanism of miniemulsion *e*ATRP. (A) Dual catalysis with one hydrophilic and one hydrophobic catalyst; (B) ion-pair and interfacial catalysis with a single hydrophilic catalyst.

Ion-pair and interfacial catalysis. A second procedure was developed where the electrochemical stimulus was delivered to the polymerizing droplets with a single catalyst complex.[63] It was determined that the hydrophilic Cu/TPMA—when combined with an anionic surfactant—could control a miniemulsion *e*ATRP without a hydrophobic partner. In the presence of sodium dodecyl sulfate (SDS, 18 wt% with respect to BA monomer) this catalytic system populated both aqueous and organic phases: 95% of $\mathrm{Br{-}Cu^{II}/TPMA^{+}}$ was bound to the interface of monomer droplets ($\mathrm{X\text{-}Cu^{II}L_{bound}}$), 1% was inside the droplets as neutral hydrophobic ion pairs $\mathrm{Br{-}Cu^{II}TPMA^{+}}$/(dodecyl sulfate)$^{-}$, and 4% was in the aqueous suspension medium. Therefore, this catalyst controlled an ATRP both from the interface and from inside the monomer droplets (**Scheme 2A**). The working electrode could effectively reduce and regenerate the catalyst that then distributed both in continuous phase and dispersed phase.

Miniemulsion *e*ATRPs with $\mathrm{Br{-}Cu^{II}TPMA^{+}/SDS}$ produced PBA with $Đ < 1.2$. Retention of chain-end functionalities allowed *in situ* chain extension to prepare block copolymers. Remarkably, crashing the miniemulsion at the end of polymerization yielded a polymer with very low copper contamination (≤ 10 mg Cu/kg polymer) because 99% of hydrophilic $\mathrm{Br{-}Cu^{II}/TPMA^{+}}$ remained in the aqueous phase. This approach was later extended from electrochemical to chemical reactivation techniques, whereby slow external addition of ascorbic acid was used to reduce $\mathrm{Cu^{II}}$ species via ARGET ATRP.[95] Excellent control of butyl acrylate (BA) and butyl methacrylate (BMA) polymerization was obtained, with as little as 0.3 mg Cu/kg polymer (i.e., 300 ppb) in the final product.

2.3 Applications

Challenging monomers and solvents. External modulation of E_{app} offered unprecedented control in an ATRP in water, a solvent characterized by the presence of an unstable X-$\mathrm{Cu^{II}}$ bond and by the generation of extremely reactive $\mathrm{Cu^{I}}$ complexes[96], in comparison with an ATRP in organic solvents.[97] In aqueous *e*ATRP, control was enhanced by slow regeneration of $\mathrm{Cu^{I}/L^{+}}$, achieved by applying a relatively positive E_{app} during polymerization of hydrophilic monomers.[48, 64]

One of the major benefits of external ATRP regulation was that electrochemical reduction of the Cu(II) catalyst was substantially independent of changes in the reaction conditions, such as temperature, pH, or chemical reactivity/composition of the reagents. For example, polymerization of acrylamide required reduced temperature of 0 °C to limit side reactions such as solvolysis of the C−Br bonds and/or competitive complexation of Cu(I) by polymer chains. However, efficient electrochemical reduction of $\mathrm{Cu^{II}}$/tris[2-(dimethylamino)ethyl]amine ($\mathrm{Me_6TREN}$) catalyst was obtained at a Pt working electrode and the reduction process was unaffected by temperature.[98]

Direct polymerization of methacrylic acid (MAA) was hampered by a side reaction involving displacement of the chain end by carboxylates.[62, 99] This side reaction was suppressed by carrying out the polymerization at pH ≤1 and switching from C-Br to C-Cl chain end. Again, application of an external electrochemical regulation allowed efficient reduction of Cu(II) despite the change of chain-end reactivity and the low pH conditions.[62, 100] In contrast, these changes altered the redox properties of chemical reducing agents such as ascorbic acid.

Polymer architecture. *e*ATRP was successfully used in the preparation of polymers with complex architecture that required high chain-end fidelity and low coupling between multifunctional macromolecules. Manipulation of E_{app} allowed selecting the best compromise between fast polymerization and low degree of radical termination in the preparation of block copolymers,[101-103] multiblock copolymers,[104] and star polymers, [105-108] even when using very low catalyst loadings, 10 ppm.[101]

*e*ATRP was particularly advantageous for the synthesis of star polymers using macroinitiators via the arm-first approach (**Figure 5A**). A linear poly(ethylene oxide)-Br (PEO-Br) macroinitiator was chain-extended with a diacrylate monomer, which crosslinked forming the star core. E_{app} was progressively shifted towards more reducing values during the polymerization, as shown in **Figure 5B**. This caused a gradual increase in the R_p, thus diminishing star–star coupling in the initial stages of the chain extension/crosslinking, providing high molecular weight (MW) stars in higher yields than with a single-potential approach.[109]

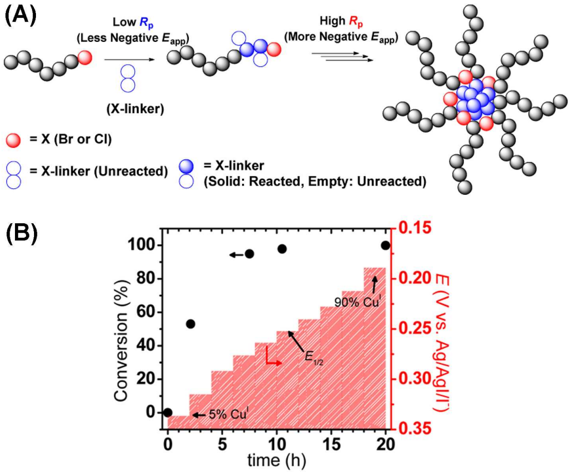

Figure 5. (A) Synthesis of PEO star polymers using multi-step E_{app}, and (B) cross-linker conversion and E_{app} versus time. Reproduced from reference [108] with permission from American Chemical Society, copyright 2013.

Surface-initiated eATRP. Surface-initiated (SI)-*e*ATRP was developed to grow polymers from initiator-functionalized surfaces. The substrate for polymer growth was either the working electrode itself (**Figure 6a**) or a nonconductive surface located close to a traditional flat (**Figure 6b**) or a bipolar electrode (**Figure 6c**).

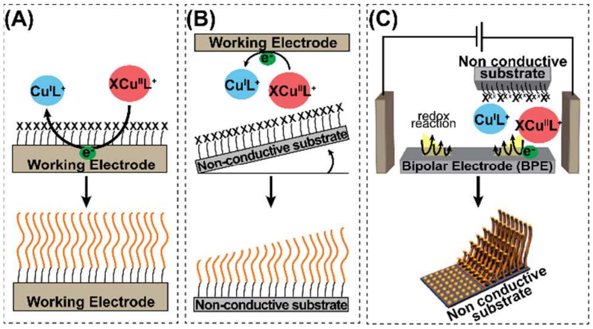

Figure 6. SI-*e*ATRP setups. (a) Polymer brushes grafted from the surface of the working electrode. (b) Gradient brushes on a non-conductive substrate. (c) 3D gradient brushes on a non-conductive

substrate by means of a bipolar electrode. Reproduced from reference [57] with permission from Elsevier, copyright 2018.

The first method (**Figure 6a**) was used to generate polymer brushes on a gold electrode, decorated by a self-assembled monolayer (SAM) of ATRP initiators.[109] Better film morphology was obtained when diluting the insulating layer of initiators with conductive naphtanethiols. The E_{app} value modulated the thickness of polymer chains. Au was the most used substrate both in organic[110, 111] and aqueous media,[112-114] but brushes were also grown from functionalized carbon fibers,[115] paraffin-impregnated graphite,[116] conducting polymers,[117] ordered mesoporous carbons,[118] Au nanodendrites,[119] and Pt wire functionalized with an enzyme.[120] Several of these modified surfaces were used as electrochemical sensors with unprecedented sensitivity and linear range. Brush growth on gold electrodes was monitored *in situ* by atomic force microscopy[121] and by electrochemical surface plasmon resonance.[122]

The second approach (**Figure 6b**) employed insulating silica layers,[109, 123] nanoparticles[124], and polyethersulfone membranes.[125, 126] This approach allowed precise spatial control: (co)polymer brushes with a gradient of thickness across a surface were grafted from a tilted, functionalized substrate placed near the electrode.[109] The tilted geometry generated a non-uniform diffusion gradient, which resulted in a gradient of the $[\mathrm{Cu^{II}}]/[\mathrm{Cu^{I}}]$ ratio across the substrate surface, causing faster brush growth close to the electrode.

A variation of this second approach used a bipolar electrode (BPE) to modulate polymerization rate along a surface (**Figure 6c**).[127] A bipolar electrode is a wireless electrode whose potential was regulated though a second set of “drive” electrodes placed outside the working solution.[128] 3D gradient polymer brushes were created on an initiator-modified glass plate located close to the cathodic region of the BPE, where reduction to $\mathrm{Cu^{I}}$ occurred at a variable rate according to the potential gradient across the electrode. A small BPE (~1 mm) with cylindrical geometry was used to “write” polymer brushes on a surface as an excellent illustration of spatial control.

2.4 *e*RAFT

An electrochemically mediated reversible addition-fragmentation chain transfer polymerization (*e*RAFT) presented different challenges than an *e*ATRP. While Cu/L complexes for ATRP had a well-defined and reversible redox behavior,[29, 129] RAFT agents gave irreversible peaks (**Figure 7B**).[130]

These irreversible redox processes could not be directly exploited to generate radicals. Essentially, the chain transfer agents were decomposed upon reduction.[131, 132] To circumvent this limitation, various radical initiators, such as benzoyl peroxide (BPO), or diazonium salts, such as 4-bromobenzenediazonium tetrafluoroborate ($BrPhN_2^+$), were reduced at the working electrode. A proposed mechanism of *e*RAFT is presented in **Figure 7A**.

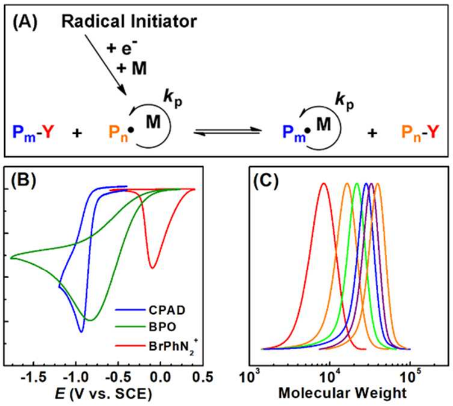

Figure 7. (A) Proposed mechanism of eRAFT. (B) Cyclic voltammetry of the chain transfer agent 4-cyano-4-(phenylcarbonothioylthio)pentanoic acid (CPAD), BPO, and $BrPhN_2^+$. (C) GPC traces during *e*RAFT polymerization of BA initiated by $BrPhN_2^+$. Reproduced from reference [130] with permission from the American Chemical Society, copyright 2017.

The reduction peak of BPO on a Pt electrode partially overlapped with that of the chain transfer agents, limiting the available range of E_{app} (**Figure 7A**).[133] However, well-controlled PBA and poly(methyl methacrylate) PMMA were obtained at E_{app} more positive than the peak potential of the chain transfer agent. Reduction of $BrPhN_2^+$ occurred at much more positive potentials than reduction of the chain transfer agents (CTAs), resulting in a more effective generation of radicals to initiate a RAFT polymerization. However, electrode conductivity was decreased by undesired electrografting of the aryl radicals on the electrode surface. The rate of radical generation was successfully controlled by electrical current or potential, providing well-defined polymers with variable degrees of polymerizations (DP) and good retention of chain-end functionality.

III. PhotoATRP

3.1 Cu systems

3.1.1 In the presence of photoinitiators and photosensitizers

Photoinitiators and photosensitizers are photoresponsive compounds, which provide reactive species, either free radicals or ions, under ultraviolet-visible (UV-Vis) light irradiation. Photoinitiated systems can be separated into two categories based on the mechanism employed to form a radical: unimolecular dissociation (type I) or a bimolecular process (type II), **Scheme 3**. A unimolecular photoinitiator produces active free radicals by homolytic bond cleavage, while a bimolecular photoinitiator system provides free radicals by the reaction between a long-lived excited triplet state of the photoinitiator and a co-initiator via a hydrogen abstraction or an electron-transfer mechanism. The active free radicals generated from photosensitive compounds could (re)generate the ATRP activator in a lower oxidation state, from a deactivator in a higher oxidation state. Many photosensitive compounds including unimolecular radical initiators,[134-137] bimolecular radical initiators,[134, 138] dyes,[136] semiconducting nanoparticles,[135, 139-143] and metal carbonyls[144] were investigated for photoinitiation and control of an ATRP process (**Figure 8**).

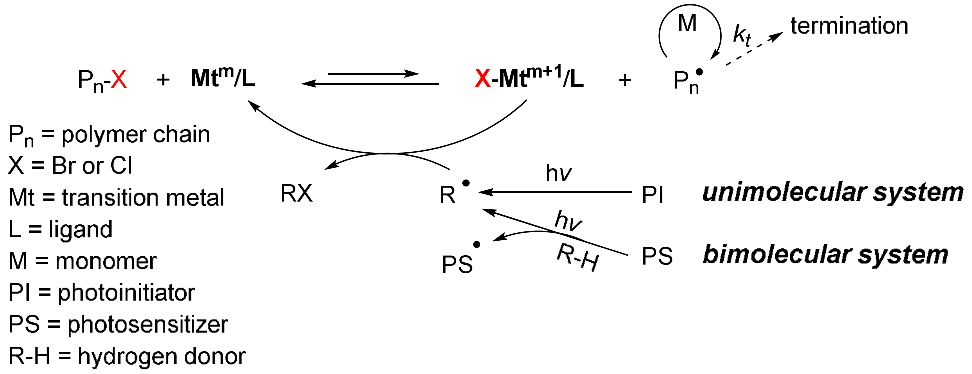

Scheme 3. Proposed mechanisms for photoATRP using unimolecular or bimolecular photoinitiating systems.

Unimolecular photoinitiators such as 2,2-dimethoxy-2-phenyl acetophenone, Irgacure 2959, and bis(2,4,6-trimethylbenzoyl)phenylphosphine oxide[145] generate free radicals via homolytic bond cleavage under UV irradiation, a procedure that could be used to establish and maintain an ATRP equilibrium at room temperature. In a bimolecular initiation system, benzophenone or camphorquinone require the presence of a co-initiator such as tertiary amines, thiols, or alcohols to produce reactive radicals for activation of an ATRP. For example a combination of camphorquinone and benzhydrol was used;[138] upon irradiation, the excited camphorquinone abstracted a hydrogen from benzhydrol to form two ketyl radicals, which reduced Cu(II) to Cu(I) rather than initiate the polymerization by addition to the monomer. In the absence of the hydrogen donor source, benzhydrol, the process was poorly controlled. The addition of benzhydrol provided good control, giving polymers with predicted molecular weight and narrow molecular weight distributions. Both reverse ATRP[146] and simultaneous reverse & normal initiation (SR&NI)[147] procedures were investigated for photoinduced ATRP.[138]

Some inorganic photoinitiators, including zinc oxide,[140] titanium dioxide,[139, 143] niobium pentachloride ($NbCl_5$),[142] and mesoporous carbon nitride nanoparticles,[135] are capable of absorbing visible light and consequently releasing electrons in the conductive band. These electrons could efficiently modulate an ATRP process by reduction of Cu(II) deactivators to Cu(I) activators.

Another type of photosensitive compound, dimanganese decacarbonyl ($Mn_2(CO)_{10}$), homolytically decomposed to form manganese pentacarbonyl radicals ($^{\bullet}Mn(CO)_5$) under visible light or sunlight irradiation.[144] These radicals abstracted halogen atoms from alkyl halides to generate carbon centered radicals, which reduced the Cu(II) deactivators to Cu(I) activators. Photoinduced ATRP of (meth)acrylates and styrene (Sty) were successfully conducted using this activation mechanism, with complete temporal control. This approach was extended to synthesize graft copolymers from commercially available poly(vinyl chloride).

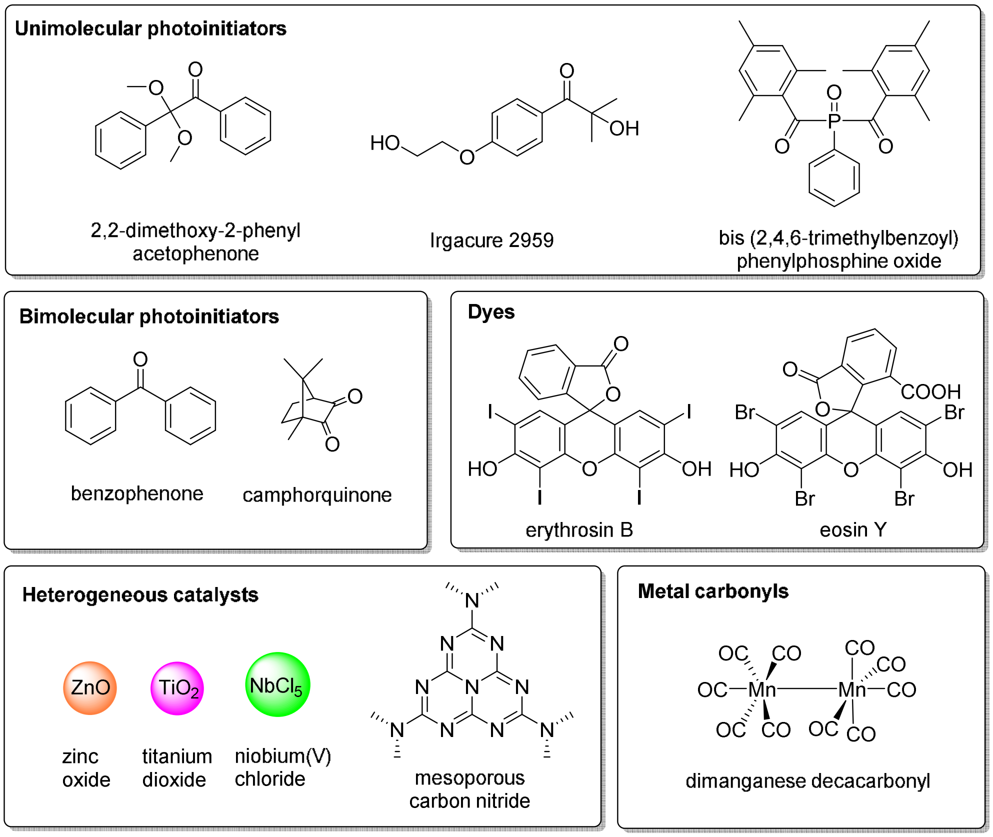

Figure 8. UV and visible light sensitive compounds used in photoinduced ATRP.

3.1.2 ATRP in the absence of photoinitiators and photosensitizers

The photoATRP in the absence of photoinitiators and photosensitizers has received increasing attention. Rate enhancement in the presence of visible light during ATRP of methyl methacrylate (MMA) with CuCl/2,2'-bipyridine (bpy) as catalyst was first observed in 2000.[148] Subsequently, UV-irradiated dithiocarbamate in the presence of copper catalyst provided a well-controlled polymerization of MMA.[149] A photoATRP (**Scheme 4**) was conducted via photo-reduction of Cu(II) salts by excess of PMDETA.[150, 151] This methodology was further developed by decreasing catalyst loading to less than 100 ppm using PMDETA and TPMA ligands.[152, 153] Later, a Cu-based photoATRP was reported for polymerization of acrylates in the presence of excess of Me_6TREN ligand.[154, 155]

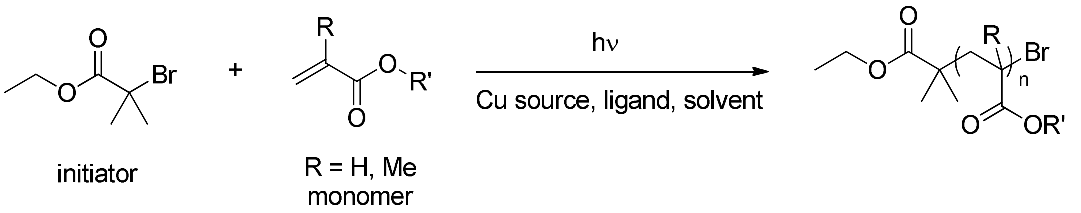

Scheme 4. General reaction scheme for a photoATRP reaction with Cu as catalyst and excess ligands.

Initiators. Alkyl halides initiators play a crucial role in ATRP reactions. PhotoATRP reactions carried out in the absence of an ATRP initiator only resulted in uncontrolled polymerizations and low conversion of monomers.[135, 151-158] Ethyl α-bromoisobutyrate (EBiB) was the most frequently used initiator for photoATRP of acrylates, while 2,3-dihydroxypropyl 2-bromo-2-methylpropionate and 2-(2-hydroxyethoxy)ethyl 2-bromo-2-methylpropionate were also successfully used as ATRP initiators under photoATRP conditions (**Figure 9**). Bifunctional initiators, ethylene bis(2-bromoisobutyrate) and bis[2-(2'-bromoisobutyryloxy)ethyl]disulfide, were used to synthesize α,ω-telechelic block copolymers.[159]

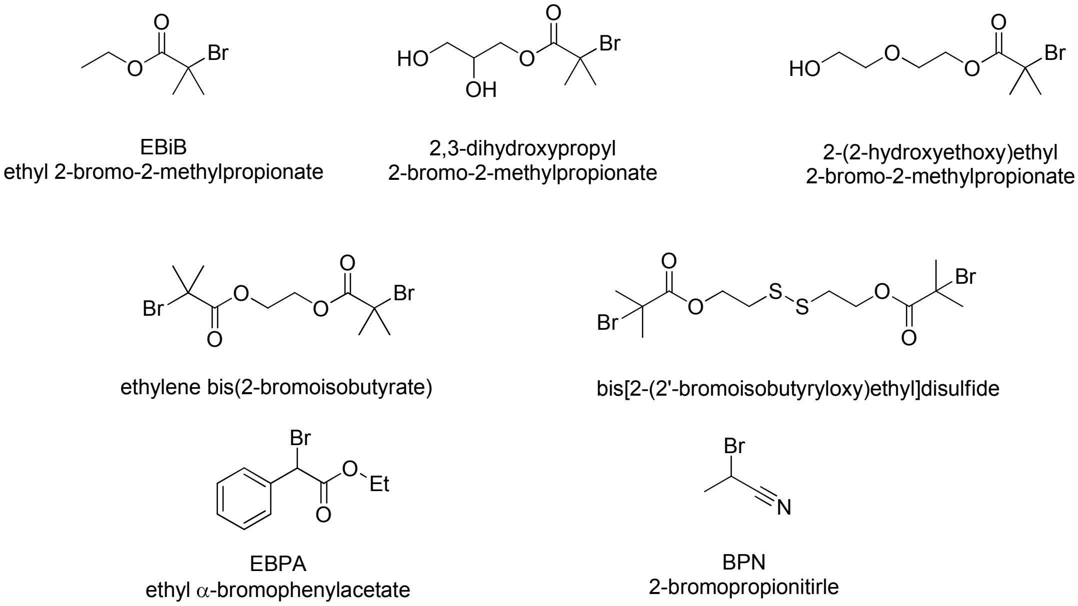

Figure 9. Initiators used in photoATRP reactions using Cu as catalyst and excess ligands.

Ethyl α-bromophenylacetate (EBPA) and 2-bromopropionitrile (BPN) were typically selected as more reactive initiators for polymerization of methacrylates,[160] providing polymers with lower dispersity compared to the polymerizations of methacrylates using EBiB as initiator.[152, 153] Chlorinated initiators were less active under photoATRP conditions, leading to a slower rate of polymerization and poorer control due to lower initiation efficiency compared to alkyl bromides.[161, 162]

Copper salts. The copper source and selection of ligands are important parameters in photoATRP reactions, due to the solubility of formed copper complexes and the possibility of photo-reduction of the Cu(II) complex by excess ligands. Most photoATRP systems used copper(II) bromide as the copper source, and resulted in good control over the polymerization of various monomers in the presence of different solvents and various light sources.[154, 156, 163-166] However, in addition to $CuBr_2$ as the sole source of copper, copper (0), copper (I) bromide, and copper (II) chloride were used as the copper salts.[154] Also, copper formate,[166] copper(II) gluconate,[167] CuO,[156] and $CuSO_4 \cdot 5H_2O$[161] were successfully used. Thus, whatever copper source was employed, the polymerization was controlled by the $CuBr/CuBr_2$ species formed *in situ*.

Cu-MOF. A solid-state catalyst based on a copper metal organic framework (MOF) was developed for photopolymerization under visible light, without requiring external photoinitiators or sensitizers.[168] The MOF, composed of terephthalic acid linkers and amine ligand pillars, was reduced from the Cu(II) to the Cu(I) state by simple visible light irradiation. Challenging monomers such as vinylpyridines, which can strongly complex to soluble Cu ions, were successfully polymerized due to the stability of the MOF crystal structure. Moreover, as a heterogeneous catalyst, the MOF was easily separated, recovered, and repeatedly used for several photopolymerizations.

Ligands. PhotoATRP of methyl acrylate (MA) with EBiB as ATRP initiator using tris(2-aminoethyl)amine (TREN) as ligand provided a similar degree of control to the polymerization using Me_6TREN (**Figure 10**). However, the polymerization with PMDETA resulted in a slower polymerization as well as inferior control.[154] TPMA and tris((4-methoxy-3,5-dimethylpyridin-2-yl)methyl)amine (TPMA*3) were used as ligands for photoATRP of both acrylate and methacrylate in dimethylformamide (DMF) with visible light irradiation.[153] The polymerizations with these ligands provided very narrow molecular weight distributions with only 100 ppm copper catalyst.

A Cu-based photoredox catalyst, $[Cu(phen)_2]Br$ (phen: 1,10-phenanthroline), was reported for photoATRP using visible light.[169, 170] Although the polymerization was very slow, due to the very low light intensity of a 0.9 W light-emitting diode (LED, λ = 465 nm) light source, the polymerization provided excellent control with only 80 ppm catalyst.

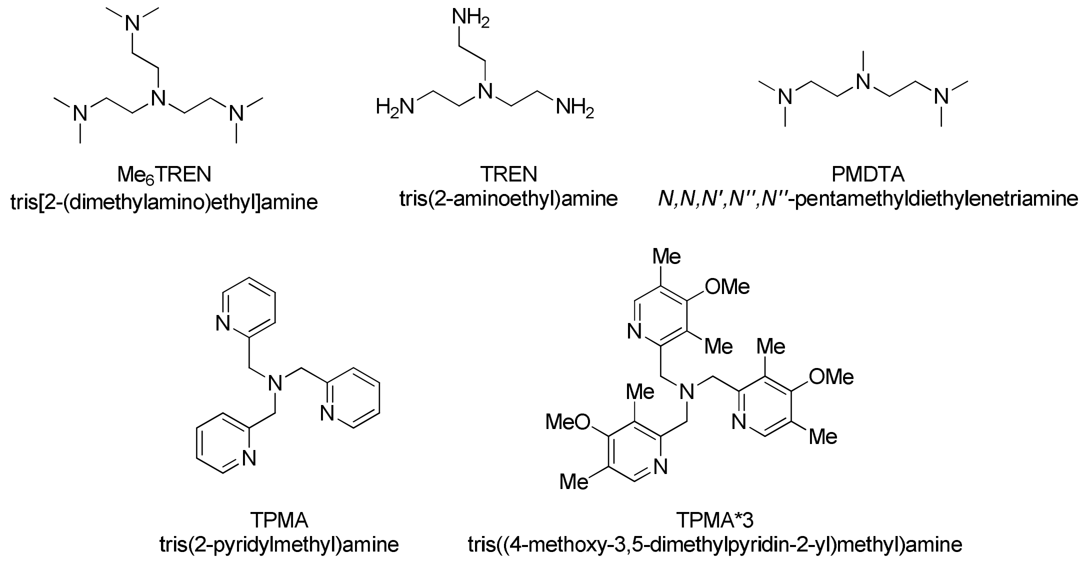

Figure 10. Examples of ligands investigated in photoATRP.

Solvents. Two parameters are crucial for selection of a suitable solvent for a photoATRP: solvent polarity and ability to dissolve the copper complex. For example, bulk polymerization of MMA did not provide a good control over the polymerization due to insufficient solubility of the copper complex in the non-polar medium.[161, 164] Much better control was obtained when methanol was added to the reaction mixture to increase the solubility of catalyst.[150] Most photoATRP reactions of acrylates were performed in dimethyl sulfoxide (DMSO).[135, 154-156, 163-167, 171-173] Other suitable solvents included ionic liquids,[163] acetonitrile (MeCN),[135, 154] DMF,[153, 154, 164] toluene, and alcohols.[154, 164] PhotoATRP of methacrylates was predominantly conducted in DMF,[141, 153, 157, 161, 172] but successful polymerizations were also carried out in DMSO,[156, 161] anisole,[152, 156, 161] acetonitrile,[135] methanol,[150, 174], 1-butyl-3-methyl-imidazolium hexafluorophosphate ([bmim][PF_6]),[157] or bulk monomers.[135, 151] The copper-catalyzed photoATRP of semi-fluorinated (meth)acrylates was conducted in a semi-fluorinated solvent, 2-trifluoromethyl-2-propanol, which gave good monomer, polymer, and catalyst solubility, while avoiding transesterification reactions.[175]

Water was considered a challenging solvent for ATRP due to the high ATRP equilibrium constant, partial dissociation of halide ion from deactivator, and hydrolysis of carbon-halogen bond in water.

For example, polymerization of oligo(ethylene glycol) methyl ether acrylate ($OEGA_{480}$) in water resulted in an uncontrolled free radical polymerization under photoATRP conditions,[164] while the same reaction in DMSO gave well-defined polymers. Recently, a successful photoATRP in aqueous media was reported for the polymerization of oligo(ethylene oxide) methyl ether methacrylate (OEOMA) using $CuBr_2$/TPMA as catalyst.[176] TPMA was selected as ligand because it formed a stable Cu(I) complex without significant disproportionation.[64] Good control was obtained with Cu concentrations as low as 22 ppm after addition of 5 or 30 mM NaBr to the reaction mixture. A similar approach was later reported for photoATRP of water-soluble oligo(ethylene oxide) methyl ether acrylate (OEOA).[177]

Irradiation and temporal control. The source of irradiation has a significant impact on photoATRP reactions, since different copper complexes and reaction mixtures have different absorption spectra. Various light sources were investigated for the polymerization of MA with 100 ppm $CuBr_2$ and TPMA*3 as ligand in DMF (**Figure 11**).[153] An attempt to conduct a polymerization using red light (λ = 631 nm; 8.9 ± 0.5 mW/cm²) gave no conversion after more than 20 hours of irradiation, since the copper complex did not absorbed at this wavelength. However, irradiation within the ligand-to-metal charge-transfer (LMCT) region by blue (λ = 450 nm; 10.0 ± 0.5 mW/cm²) and violet (λ =392 nm; 0.90 ± 0.05 mW/cm²) light resulted in 26% and 71% conversion after 20.5 h and 27 h, respectively. Sunlight-mediated polymerization was even more efficient, reaching 81% conversion and providing a well-defined polymer with M_n = 21,000 and $Đ$ = 1.09.

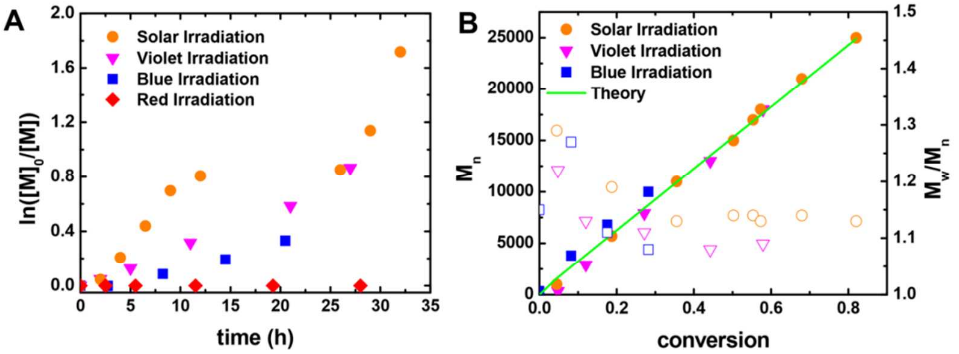

Figure 11. (A) Kinetics and (B) M_n (solid points) and M_w/M_n (open points) evolution in the polymerization of MA using different radiation sources. Conditions: [MA]:[EBiB]:[$CuBr_2$]:[TPMA*3] = 300:1:0.03:0.135 in 50 vol% DMF at room temperature. Reproduced from Ref. [153], copyright 2012 with permission from the American Chemical Society.

Different light sources were also examined for a Cu-based photoATRP of MA using Me$_6$TREN as ligand and EBiB as initiator in DMSO.[154] The polymerization with UV light (360 nm) gave a significantly faster polymerization rate than sunlight or visible light. This was attributed to the larger absorption coefficient of Cu complexes in the UV range compared to the visible range. In agreement with previous studies,[153] photoATRP mediated by blue light gave a slower polymerization rate but maintained good control.[154]

Temporal control is one of the major advantages of photomediated reactions over thermal reactions. In principle, no reaction should occur without irradiation, and the reaction should stop when the irradiation is turned off (**Figure 12**). However, limited temporal control could be achieved in some photoATRP reactions—in the absence of irradiation the polymerization rate was much slower, but the reaction did not fully stop. [153] These observations indicated that the photogenerated active Cu(I) activator remained in the reaction mixture and continued to activate the dormant species without irradiation.

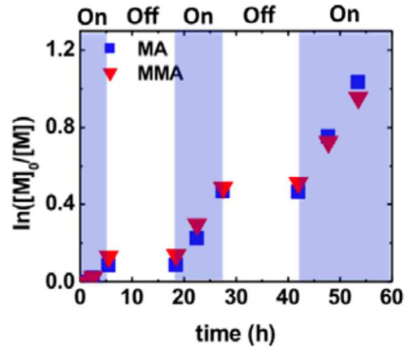

Figure 12. Kinetics for the polymerization of MMA and MA with "on/off" periods. Conditions: [MA]/[EBiB]/[CuBr$_2$]/[TPMA*3] = 300:1:0.03:0.135 or [MMA]/[EBPA]/[CuBr$_2$]/[TPMA] = 300:1:0.03:0.135, 50 vol % DMF, at room temperature with 392 nm radiation. (Reproduced from Ref. [153], copyright 2012 with permission from the American Chemical Society.)

3.1.3 Mechanism: regeneration vs. activation

The mechanism of photoATRP was investigated in several reports.[153-155, 178] Photoirradiation does not change the rate of chain-end activation by traditional ATRP copper complexes: the rates of activation of alkyl halides by Cu^I/*N*,*N*,*N*`,*N*``,*N*```,*N*```-hexamethyltriethylenetetramine (HMTETA) or TPMA catalyst were measured under irradiation and negligible differences were found compared to the rates without irradiation.[149, 153] The $CuBr_2$ complex with excess TPMA or Me_6TREN ligands or with triethylamine under irradiation conditions could regenerate the Cu(I) activator in a reductive quenching cycle (**Scheme 5**). Excess amine was required to close the quenching cycle: low monomer conversion was obtained in the polymerization of MA conducted in the absence of free ligand, with $CuBr_2:Me_6TREN = 1:1$ under 392 nm irradiation. A faster rate of polymerization was observed after increasing the ratio of ligand to copper.[155] An appropriate electron donor such as trialkylamine could be added to the reaction to replace the excess amount of ligand, maintaining similar kinetics with good polymerization control. In contrast, the ground state of catalyst $[Cu(phen)_2]Br$ was not reactive enough to activate alkyl halide and conduct a thermal copper-mediated radical polymerization at room temperature. However, upon irradiation, the excited $[Cu(phen)_2]^{+*}$ reduced the alkyl halide to initiate the polymerization and generated a propagating radical by an oxidative quenching cycle rather than an amine-based reductive quenching cycle. [169]

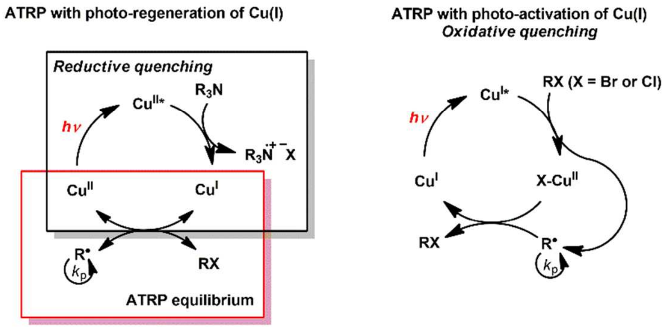

Scheme 5. Simplified mechanism for Cu-mediated photoATRP involved in an oxidative quenching cycle ($[Cu(phen)_2]Br$) or a reductive quenching cycle (e.g. $Cu(TPMA)Br_2$ or $Cu(Me_6TREN)Br_2$).

A series of polymerizations was conducted with one or more reaction components removed from the standard model reaction in order to provide a better understanding of the mechanism of photoATRP in presence of excess ligands.[155] The contribution of different pathways to activator regeneration is shown in **Figure 13** for an irradiation wavelength of 392 nm. The dominant activation (re)generation mechanism, 90%, was the photoreduction of Cu^{II} complexes by free amine moieties (Cu+L), similar to an ARGET ATRP process. The aliphatic amine was oxidized to the corresponding radical cation, which could initiate new chains after proton transfer. The second dominant contribution, 8%, to radical generation was a photoreaction between ligand and alkyl halide (RX+L), generating radicals in an ICAR-like process. This pathway was one order of magnitude slower than photoreduction of Cu(II). Other processes, such as the reaction between ligands and monomers (M+L), and the photochemical cleavage of alkyl halides (RX) were present but with negligible contribution, ~1%.

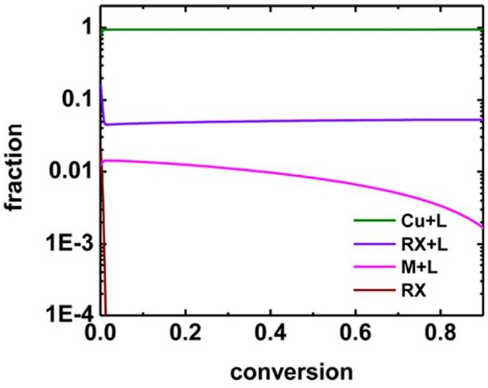

Figure 13. Fraction contributions of activator regeneration from each reaction considered for the simulated polymerization under the conditions $[MA]_0$:$[EBiB]_0$:$[Cu^{II}Br_2/L]_0$:$[L]_0$ = 300:1:0.03:0.15 in DMSO, [MA] = 7.4 M at 25 °C under 392 nm irradiation (0.9 mW/cm^2). RX is expressed here by the sum of initiating and macromolecular alkyl halides. Reproduced from [155], copyright 2014 with permission from American Chemical Society.

A more detailed investigation, at the molecular level, was conducted using a pulsed-laser polymerization (PLP) technique in conjunction with electrospray-ionization mass spectrometry (ESI-MS) to analyze the structure of the polymer and its chain end groups.[178] Similar to the previous study,[155] different combinations of the photoATRP reaction components were examined—EBiB, $CuBr_2$, Me_6TREN, MMA, and DMSO.[178] This work confirmed that the contribution of amine-containing Me_6TREN is the dominant activation pathway in the photoreduction of $CuBr_2/L$. Different irradiation sources can affect the contributions from different pathways. For instance, homolytic cleavage of C-Br bond should be faster with UV light than with visible light.

The effect of light on normal, ICAR, and ARGET ATRP was investigated.[158] ICAR ATRP was not significantly influenced under irradiation with two fluorescent lamps (λ = 400-750 nm) at a distance of 10 cm from the reaction mixture.[179] However, in the presence of very low concentration of 2,2'-azobis(2-methylpropionitrile) (AIBN), 0.035 equiv. with respect to ATRP initiator, a photochemical process contributed *ca.* 50% to activator regeneration in a 392 nm photoreactor (0.9 mW/cm^2).

An ARGET ATRP with excess PMDETA ligand gave similar polymerization rates under both ambient light and dark conditions.[180] Under normal ATRP conditions a large enhancement in polymerization rate was observed under ambient light compared to the polymerization in dark. This enhancement in rate could be due to photoreduction of the Cu(II) complex by excess ligands. However, in the ARGET ATRP, the photoreduction process was plausibly much slower than the chemical reduction of Cu(II) by reducing agents such as ascorbic acid.

3.2 Fe systems

Iron is another well-studied transition metal for ATRP due to its abundance, lower toxicity, and lower cost than copper.[181-188] Photomediated ATRP using iron as catalyst successfully polymerized various methacrylates, while polymerization of acrylates was more challenging. Under photoICAR (PhICAR) conditions with BPO and AIBN as photoinitiators, a controlled radical polymerization of MMA was achieved using CCl_4 as the ATRP initiator and $FeCl_3$/tetramethylethylenediamine (TMEDA) as catalyst.[189] Moreover, $FeCl_3$/bpy complex was reduced in ethanol under irradiation at room temperature,[190] and a well-defined PMMA was synthesized using this photoreduction process. An induction period was typically observed due to slow formation of the Fe(II) activator *in situ*, and complete temporal control was observed when the irradiation was turned off.

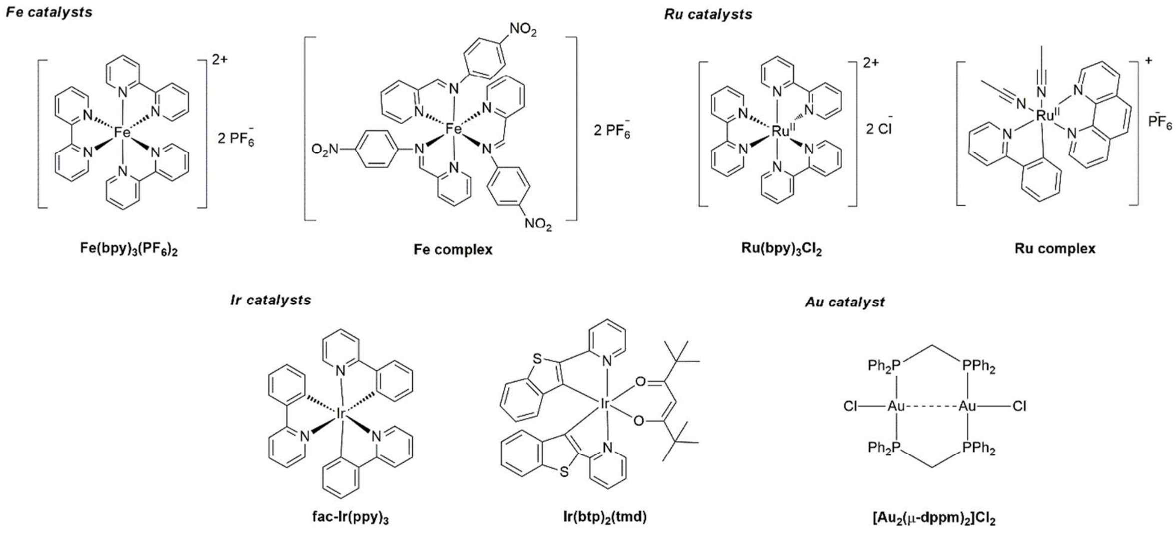

Figure 14. Structures of selected Fe, Ru, Ir and Au catalysts in photoATRP.

PhotoATRP of MMA based on $FeCl_3$/triphenylphosphine (PPh_3) as catalyst was also conducted with nanosized α-Fe_2O_3 as photoinitiator in poly(ethylene glycol) (PEG) as solvent.[191] The polymerization was not perfectly controlled with the dispersity of the synthesized polymers ranging from 1.39 to 1.68. A similar situation was also observed in a photoATRP using iron-based photoredox catalysts such as $Fe(bpy)_3(PF_6)_2$[192] and the pyridylimine Fe complex shown in **Figure 14**.[193] Both catalysts gave linear semilogarithmic plots and linear relationships of M_n with conversion. However, the polymer synthesized from $Fe(bpy)_3(PF_6)_2$ had about 10 times higher molecular weight than the theoretical value, indicating a very limited initiation efficiency. A broad molecular weight distribution (M_w/M_n = 1.5 - 2.2) was observed for the polymerization with the pyridylimine Fe complex, which was attributed to the photo-degradation of the iron photoredox complexes during the polymerizations.

Based on a previous report that $FeBr_2$ could catalyze ATRP of methacrylates in the presence of polar solvents such as DMF and MeCN without additional ligands,[188] an Fe-based photoATRP of methacrylates was carried out using only air-stable $FeBr_3$ and ATRP initiators, without additional ligands, reducing agents, or thermal radical initiators.[194] A mixture containing a methacrylate monomer, $FeBr_3$, and EBPA in MeCN under irradiation provided well-defined polymers with high chain-end functionality. An ultraviolet-visible-near infrared (UV-vis-NIR) spectroscopic study showed that photoreduction of Fe(III) to Fe(II) was achieved in the presence of excess monomers under irradiation. Another interesting observation was that activation of alkyl bromide by Fe(II) activators at room temperature required irradiation, **Scheme 6**, and no observable monomer conversion was detected without irradiation. By taking advantage of this mechanism, a further simplified method was developed using only monomer and $FeBr_3$ in the absence of alkyl halide.[195] The photoreduction of $FeBr_3$ by MMA converted the monomer *in situ* to an ATRP initiator, methyl 2,3-dibromopropionate, in which only the bromine in the 2 position was an active ATRP initiator. Thus, in this system $FeBr_3$ acts as deactivator, as well as a source of the $FeBr_2$ activator and RBr initiator.

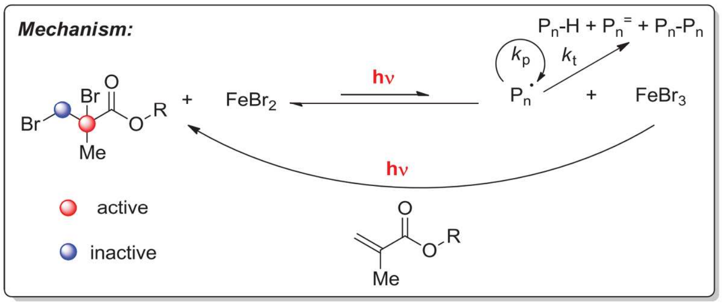

Scheme 6. Proposed mechanism of photomediated Fe-based ATRP without other additives. (Reproduced from [195], copyright 2017 with permission from Wiley)

A similar iron-catalyzed photoATRP with *in situ* formation of alkyl halide was conducted using $FeCl_3$ rather than $FeBr_3$ in the presence of tris(4-methoxyphenyl)phosphine as a ligand,[196] which was then extended to a system with low-ppm level of iron catalyst and visible light irradiation.[197] The iron catalyzed photoATRP was reported under blue light irradiation with oxygen tolerance using only ppm level of catalysts (100 – 400 ppm) in the presence of tetrabutylammonium bromide as the co-catalyst, which enabled synthesis of well-defined polymers in the presence of air.[198] A water-soluble triphenylphosphine ligand with three p-sulfonate sodium substituents, was employed to photomediate an iron-catalyzed ATRP in aqueous media.[199]

3.3 Other transition-metal based systems

Ru. Tris(bipyridine)ruthenium(II) chloride ($Ru(bpy)_3Cl_2$, **Figure 14**) is one of the often used photoredox catalysts for organic transformations. It was used as a photosensitizer in free radical polymerizations, with trimethylamine as sacrificial electron donor, already in 1985.[200] Later in 2011, a similar polymerization was conducted in the presence of EBiB using *N*,*N*-diisopropylethylamine under visible light irradiation.[201] This system efficiently polymerized various methacrylates, but not in a controlled manner.

Figure 14 also shows the structure for *cis*-[Ru(*o*-C_6H_4-2-py)(phen)$(MeCN)_2$]PF_6 (**Ru complex**), which could catalyze photoATRP with a different photo-activation mechanism.[202] The Ru complex in methanol was photosensitive and provided a reactive 16-electron Ru intermediate by dissociation of one acetonitrile ligand under visible light irradiation. The 16-electron Ru intermediate with one vacant site, behaving as an ATRP activator, provided an active radical via an inner sphere electron transfer (ISET) process with an alkyl halide. An ATRP equilibrium was established through this mechanism, which successfully polymerized MMA, BA, and Sty. Both a linear semilogarithmic kinetic plot and a linear relationship between M_n and conversion for each monomer was observed, indicating good control.

Au. A dinuclear gold (I) photoredox catalyst $[Au_2(\mu\text{-dppm})_2]Cl_2$ (dppm: (diphenylphosphino)-methane, **Figure 14**) was reported for the photoATRP of methacrylates and acrylates in the presence of EBPA as the conventional ATRP initiator under various irradiation conditions.[203] Upon irradiation $[Au_2(\mu\text{-dppm})_2]Cl_2$ formed an excited state $Au_2^{II}*$ complex ($E^{\ominus}$ = - 1.6 V vs SCE) that reduced an alkyl bromide, or a polymer bromine chain end, to provide a carbon-centered radical. The activation rate constant for the reaction between $Au_2^{II}*$ and EBPA was measured by laser flash photolysis (LFP) and a rate constant of 9.2×10^8 $M^{-1}s^{-1}$ was determined, very close to the diffusion limit for a bimolecular reaction. The oxidized form of the original catalyst, $[Au_2(\mu\text{-dppm})_2Cl_2]^+Br^-$, was detected by UV-vis spectra. Although the molecular weight distributions were broad, up to $Đ$ = 1.85, this system was considered a controlled process due to preparation of polymers with predictable molecular weight and high retention of the bromine chain end. The broad distributions could be attributed to less efficient deactivation with $[Au_2(\mu\text{-dppm})_2Cl_2]^+Br^-$, and to several side reactions that competed with the main deactivation pathway.

Ir. Similar to $Ru(bpy)_3Cl_2$, *fac*-$[Ir(ppy)_3]$ (ppy: 2,2'-phenylpyridine, **Figure 14**) is another versatile photoredox catalyst that has been used in various organic transformations [204-207], and was extended to successfully polymerize MMA, in the presence of EBPA as the ATRP initiator, under visible light.[208] This Ir-based photoATRP system featured complete temporal control, indicating that the photoexcited Ir catalyst was the true activator. The ground state of *fac*-$[Ir(ppy)_3]$ is not a strong reductant and is not able to reduce the alkyl halide. Under irradiation, however, an excited state *fac*-$[Ir(ppy)_3]*$ is formed that acts as a strong reductant ($E^{\ominus}$ = - 1.73 V vs SCE) to activate an alkyl bromide (R-Br) or polymer with bromine end (P_n-Br) to generate the initiating or propagating radical. The catalytic cycle is closed by deactivation of the propagating radical by the oxidized Ir^{IV} complex, providing the ground-state Ir complex and polymer with bromine chain end.

The Ir-catalyzed photoATRP was used to polymerize both methacrylates and acrylates, including ethylene glycol methyl ether methacrylate,[209] 1,1,1-trifluoroethyl methacrylate (TFEMA),[210] propargyl methacrylate,[211] and methyl, ethyl, *n*-butyl, and *t*-butyl acrylates.[212] It is worth noting that methacrylic acid (MAA), one of the most difficult monomers to polymerize by ATRP, due to the presence of a carboxylic acid functional group, was successfully polymerized using Ir-based photoATRP. Sufficient control was retained when polymerizing a MAA-benzyl methacrylate random block copolymer with up to 20% MAA content.[208] Acrylic acid (AA) was also copolymerized using the same catalyst in a random copolymerization with ethyl acrylate (EA).[212] The Ir catalysts could be easily separated and recycled when using 1,2-dichlorobenzene and ethanol as the co-solvent.[213] After the reaction was complete, water was added to induce phase separation and leave the Ir catalyst in the 1,2-dichlorobenzene phase for recycling.

A new iridium photoredox complex, Ir(btp)$_2$(tmd) (btp: 2-(2′-benzothienyl)pyridine; tmd: 2,2,6,6-tetramethyl-3,5-heptanedione, **Figure 14**), was synthesized to catalyze a controlled radical polymerization under mild conditions (irradiation λ: 457 – 532 nm).[214] The Ir(btp)$_2$(tmd) catalyst complex absorbs more visible light and has longer luminescence lifetimes (4400 ns) compared to *fac*-[Ir(ppy)$_3$] complex (1300 ns). A good control over polymerization of MMA was achieved using 0.14 mol% catalyst to initiator, giving polymers with predictable M_n and low $Đ$ (1.2 - 1.3).

3.4 Metal-free systems

After the successful development of photoATRP using transition-metal based catalysts, photoredox catalysts based on small organic molecules were developed to catalyze ATRP under irradiation with an oxidative quenching cycle. The concept of ATRP in the absence of transition metals, called metal-free ATRP (MF-ATRP), organocatalyzed ATRP (O-ATRP), or photoinduced electron transfer ATRP (PET-ATRP), is highly attractive due to easy purification, reduced toxicity, and no interference of catalyst residues in electronic applications or in side reactions catalyzed by transition metals.[215, 216] The catalysts have been classified mainly based on the core structure: phenothiazines (PTZ), phenazines, polynuclear aromatic hydrocarbons, and others including phenoxazines. Some catalysts undergoing reductive quenching cycle were also investigated, such as fluorescein and camphorquinone. The structures of selected catalysts are shown in **Figure 15**.

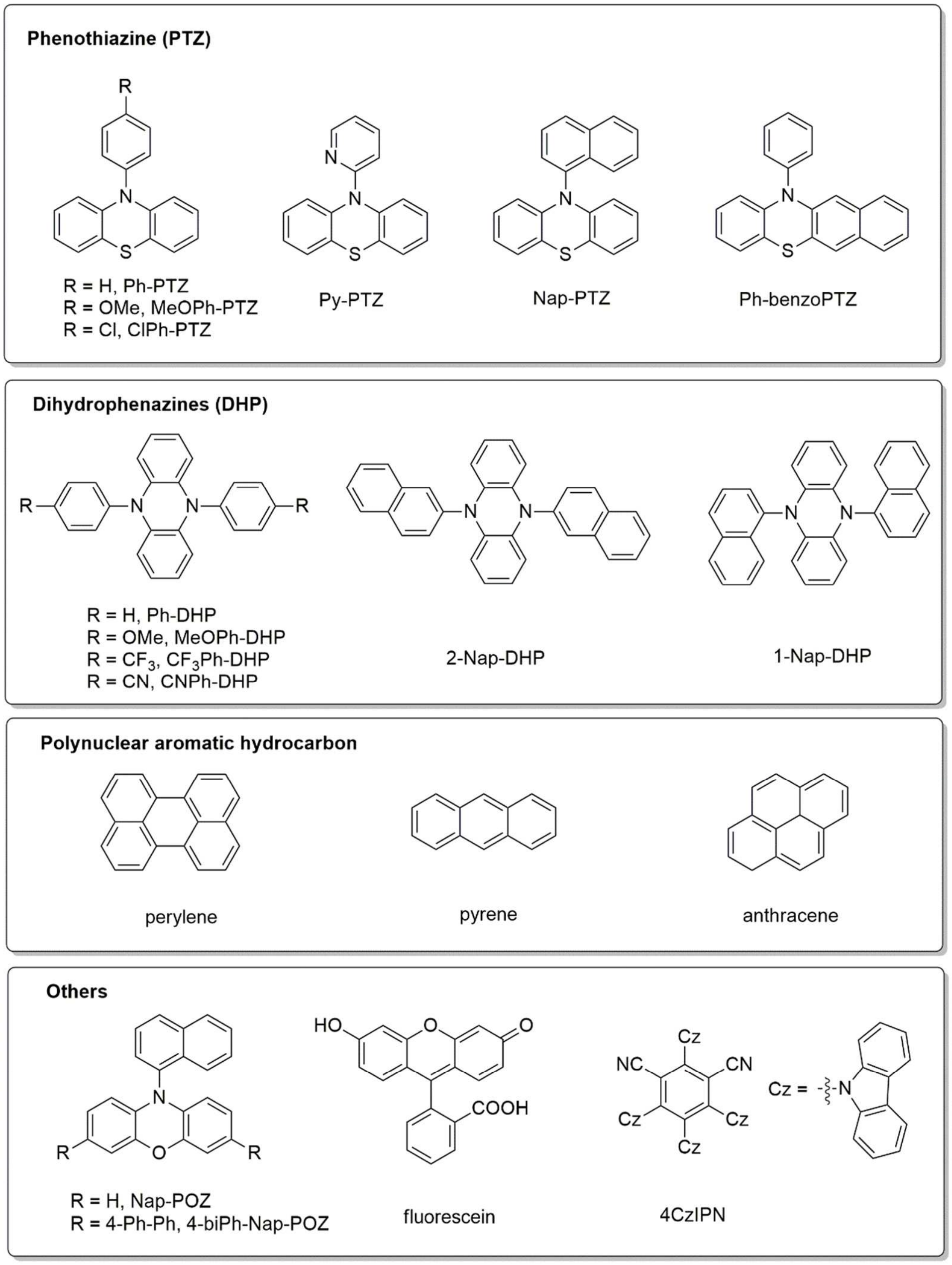

Figure 15. Structures of selected metal-free catalysts in photoATRP.

3.4.1 Phenothiazine

The first successful metal-free ATRP was achieved when 10-phenylphenothiazine (Ph-PTZ, **Figure 15**) was used as catalyst for the polymerization of MMA, benzyl methacrylate (BnMA), and dimethylamine methacrylate (DMAEMA) using 380 nm irradiation.[217] Several control experiments omitting either irradiation, initiator, or catalyst resulted in no polymerization, or in an uncontrolled polymerization. The classic behavior for a photoinduced ATRP system, such as temporal control, linear evolution of molecular weight and conversion, and linear semilogarithmic kinetic plot could be obtained using Ph-PTZ as catalyst. In comparison, the polymerization with 10-methylphenothiazine (Me-PTZ) gave partial control probably due to its instability during the reaction. The PTZ-catalyzed photoATRP system was further investigated with various ATRP initiators, irradiation sources, and different PTZ-based catalysts.[218] Consistent with other photoATRP results, a faster polymerization rate was observed when the PTZ-catalyzed photoATRP was conducted with a stronger irradiation source. The polymerization with EBiB as ATRP initiator provided broader distribution and lower initiator efficiency than the reaction with EBPA, whereas the polymerization with ethyl α-chlorophenylacetate (EClPA) gave an uncontrolled free radical polymerization. Phenyl benzo[*b*]phenothiazine (Ph-benzoPTZ) with more extended conjugation exhibited a stronger absorption in the visible light region (**Figure 16**). It successfully catalyzed metal-free photoATRP under a 392 nm visible-light LED.[219]

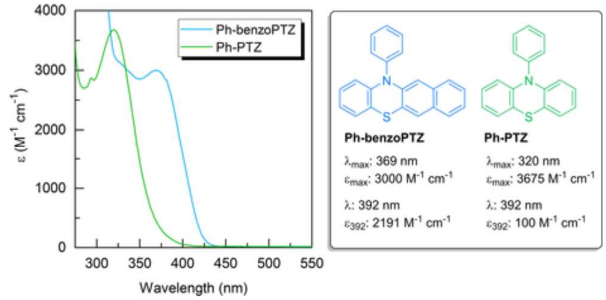

Figure 16. UV-Vis spectra of photocatalysts Ph-benzoPTZ and Ph-PTZ in dimethylacetamide (DMA) (concentration: 3.07×10^{-4} M). (Reproduced from [219], copyright 2017 with permission from Wiley.)

Metal-free ATRP with Ph-PTZ was applied to different monomers. A new type of single-ion homopolymer electrolyte was prepared via metal-free ATRP of poly(ethylene oxide) methacrylate lithium sulfonyl(trifluoromethylsulfonyl)imide, avoiding any residual transition metal.[220] The polymerization of three biomass-derived monomers including soybean oil, furfuryl, and dehydroabietic ethyl methacrylate gave good control over molecular weight and dispersity.[221] This system was also applied to polymerize acrylonitrile to produce polyacrylonitrile with different targeted molecular weights. Linear semilogarithmic kinetic plots and increasing molecular weights with conversion were observed in metal-free ATRP of acrylonitrile using Ph-PTZ as catalyst.[222] However, the M_n of the synthesized PAN was higher than the theoretical value, indicating either slow initiation or inefficient deactivation. Compared to PAN obtained by classic Cu-mediated ATRP ($M_w/M_n < 1.10$),[223, 224] metal-free ATRP gave lower degree of control. However, for some applications it could be desirable to prepare polymers without residual transition metal in the final product.[225-228]

An oxidative quenching cycle mechanism was proposed for PTZ-catalyzed metal-free photoATRP (**Scheme 7**).[218] Upon suitable irradiation, the ground state Ph-PTZ was excited to a singlet state, forming Ph-PTZ* that transferred an electron to an alkyl bromide to form a propagating radical and radical cation Ph-PTZ$^{\bullet+}$ in a dissociative electron transfer process. A report based on fluorescence and phosphorescence suggested that a triplet excited state in Me-PTZ might undergo electron transfer to an alkyl halide.[229] The fluorescence was easily observed at room temperature while phosphorescence was only detected at 77 K. Nevertheless, activation from a singlet excited state might still dominate the activation process, as suggested from evidence of PTZ-catalyzed radical dehalogenation. [230, 231]

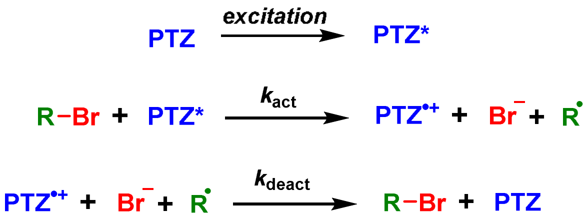
$$\mathrm{PTZ} \xrightarrow{\textit{excitation}} \mathrm{PTZ^*}$$
$$\mathrm{R{-}Br} + \mathrm{PTZ^*} \xrightarrow{k_{act}} \mathrm{PTZ^{\bullet+}} + \mathrm{Br^-} + \mathrm{R^\bullet}$$
$$\mathrm{PTZ^{\bullet+}} + \mathrm{Br^-} + \mathrm{R^\bullet} \xrightarrow{k_{deact}} \mathrm{R{-}Br} + \mathrm{PTZ}$$

Scheme 7. Proposed mechanism of PTZ-catalyzed photoinduced metal-free ATRP.

This activation pathway was identified as outer sphere electron transfer (OSET) process by application of modified Marcus theory.[232-235] Ph-PTZ* reacted with methyl 2-bromoisobutyrate (MBiB) very rapidly ($k_{act,OSET} = 5.8\times10^8$ M^{-1}s^{-1}). Furthermore, LFP was used to determine the rate constant, 5.7×10^9 M^{-1}s^{-1}, for the reaction between EBPA and Ph-PTZ*. The radical added several monomer units before being deactivated potentially by combination of Ph-PTZ$^{\bullet+}$ and Br$^-$ in a termolecular associative electron transfer process. The bromide anion interacted strongly with Ph-PTZ$^{\bullet+}$ and such a complex could also react with propagating radicals in a bimolecular deactivation process resembling Cu-based ATRP. Thus, the catalytic cycle was closed by the deactivation process that regenerated the ground state catalyst as well as the polymer with a bromine chain end. The system did not have the same level of control as the Cu-based ATRP, attributed to a slower deactivation process, as well as to the presence of some side reactions.

3.4.2 Dihydrophenazine

A visible light mediated metal-free ATRP was developed using 5,10-diaryl-5,10-dihydrophenazines (DHP) derivatives.[236] In initial studies, DHP with electron donating (-OMe), neutral (-H), and electron withdrawing (-CF_3 and -CN) moieties on the *N*-phenyl substituents were synthesized. All four phenazine compounds have sufficiently strong triplet excited-state reduction potential to reduce ATRP initiator or polymeric alkyl halides to initiate the polymerization or reform the propagating radical, respectively. The stable radical cations formed during the photoinduced electron transfer have high enough oxidation potentials to deactivate the propagating radicals. A polymerization initiated with EBPA and CF_3Ph-DHP as catalyst in DMA provided PMMA with lowest dispersity (M_w/M_n = 1.17) and highest initiation efficiency (66%) among these four catalysts. A detailed comparison and theoretical investigation among these catalysts led to the design of two more efficient catalysts, 2-Nap-DHP and 1-Nap-DHP, which resulted in more efficient control. The polymerizations of BA and AN were more challenging, resulting in formation of polymers with a higher dispersity of 1.42 and 1.70, respectively. The attempted polymerization of Sty and vinyl acetate, however, gave no monomer conversion.

The dihydrophenazine-catalyzed metal-free ATRP was proposed to undergo an oxidative quenching cycle, similar to the PTZ-catalyzed system. However, the excited state of DHP is a triplet, which possessed a significantly longer lifetime than a singlet excited state. Consequently, a longer lifetime of excited state would result in more efficient activation as well as deactivation. Essentially, a larger portion of the catalyst participated in the activation/deactivation cycles as a consequence of the longer excited state lifetimes. Further studies pointed out that photoexcited intramolecular charge transfer in *N*,*N*-diaryldihydrophenazine played an important role in minimizing fluorescence and enhancing the electron transfer between the triplet state and the substrates.[237]

Photoexcited intramolecular charge transfer was studied by measuring the emission spectra of catalysts in various solvents with different polarities. Two different excited states where observed: one showing charge transfer character, where the excited state electron was intramolecularly transferred from the phenazine core to the π* orbital of the *N*-aryl substituent; the second type of excited state was instead entirely localized on the core of the photocatalyst. The dihydrophenazines compounds with charge-transfer character, possessing naphthalene substituents, showed large Stokes shifts and red-shifted emission in more polar solvents. In contrast, the compounds that gave local excitation, such as Ph-DHP and MeOPh-DHP, had similar emission spectra in different solvents (**Figure 17**). This phenomenon was further studied by computational calculations and experiments.[238] Nevertheless, a different activation mechanism was suggested based on investigation of transient vibrational and electronic absorption spectroscopy with sub-picosecond time resolution: electron transfer from short-lived singlet excited state gave better control by suppressing the formation of excess radicals.[239]

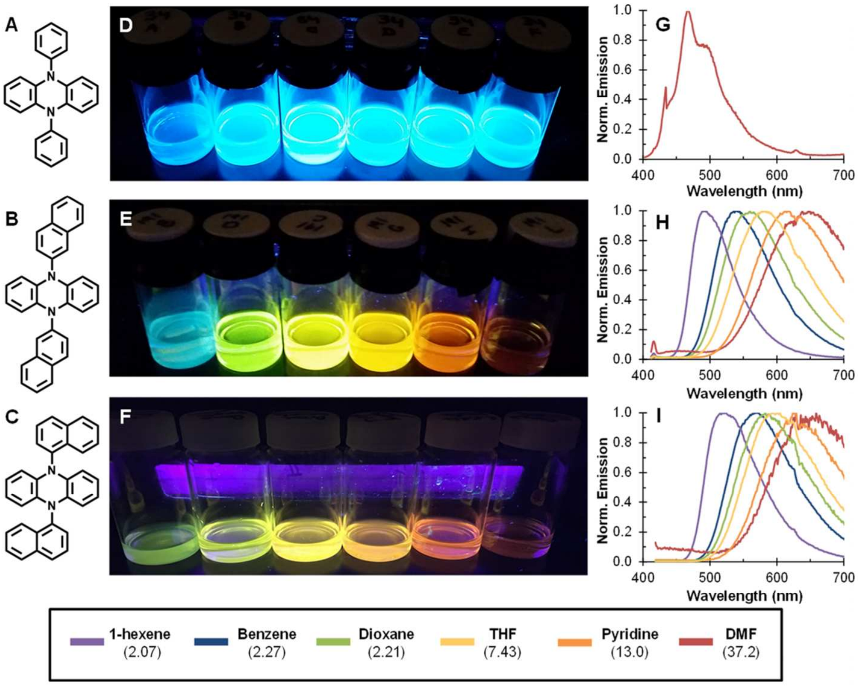

Figure 17. Diaryldihydrophenazines with local excitation (A) or charge transfer (B and C). The solutions of diaryldihydrophenazines under 365 nm irradiation (D, E, and F) and their emission spectra (G, H and I) in various solvents. (Reproduced from [237], copyright 2017 with permission from the American Chemical Society.)

3.4.3 Polynuclear aromatic hydrocarbons

In an even earlier report, perylene was investigated as an organic photoredox catalyst for the polymerization of MMA and other vinyl monomers (**Figure 15**);[240] however, the results were not satisfactory. In the presence of a conventional ATRP initiator, such as EBPA, in various solvents the polymerization with 0.11 equiv. perylene to initiator provided only 2% to 40% initiation efficiency, and the molecular weight decreased with conversion, indicating an uncontrolled radical polymerization. On the other hand, a linear semilogarithmic kinetic plot and temporal control were observed. Limited bromine chain end functionality was determined by chain-extension and MALDI-TOF. These results suggested that perylene acted as an efficient activator to generate a free radical to induce radical polymerization, but it could not generate a sufficiently stable deactivator to efficiently deactivate the radical and achieve a controlled process. This system was also used to synthesize hyperbranched polymers.[241]

A similar polymerization with anthracene was not very successful, giving polymers with bimodal MW distribution in low yields due to the [4+4] cycloaddition side reaction between excited anthracene and its own ground state.[242] Pyrene was more robust as it formed an exciplex with the excited form of pyrene rather than a [4+4] cycloadduct. Excited pyrene as well as the exciplex activated alkyl halides to alkyl radicals.

3.4.4 Other photoredox catalysts

N-Arylphenoxazines (POZ, **Figure 15**) have been synthesized and reported as a metal-free photoredox catalyst in ATRP.[243-245] Replacing the sulfur in the phenothiazine core with oxygen, as in phenoxazine, resulted in a conformation change of the heterocyclic rings (Figure **18**). The phenothiazine core had bent conformations in both ground and excited states, but a planar geometry in the radical cation state; conversely, the phenoxazine catalyst maintained a planar conformation during the catalytic cycle, which provided a lower reorganization energy compared to the phenothiazine system. The initially developed 10-phenylphenoxazine was further functionalized to improve its photoredox properties: addition of 4-biphenyl core substituents and *N*-aryl functionalization with naphthalene induced a red shift into the visible spectrum and also enhanced the molar extinction coefficient.

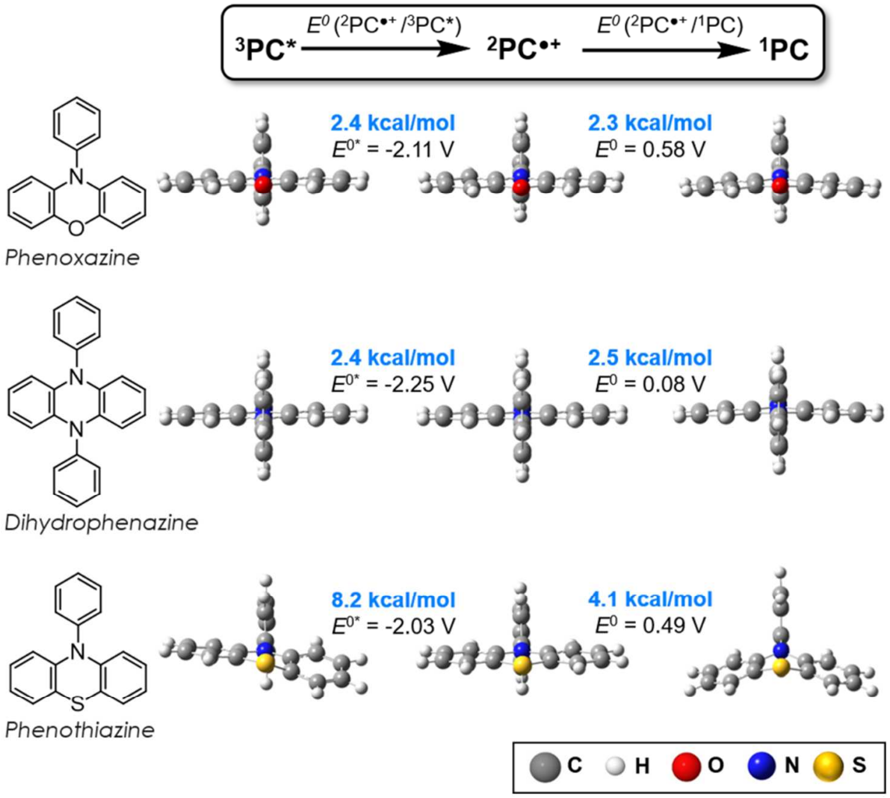

Figure 18. Geometric reorganization energies and reduction potentials (vs SCE) for 10-phenylphenoxazine, diphenyl dihydrophenazine, and 10-phenylphenothiazine (bottom) transitioning from the ^{3}PC* to ^{2}PC$^{•+}$ to ^{1}PC species involved in the proposed mechanism for photoredox metal-free ATRP. (Reproduced from[243], copyright 2016 with permission from the American Chemical Society.)

Highly conjugated electron-rich thienothiophene derivatives were used in metal-free ATRP.[246] Other highly conjugated structures were also employed: the polymerization of MMA with metal-free ATRP using ppm amount of catalyst 1,2,3,5-tetrakis(carbazol-9-yl)-4,6-dicyanobenzene (4CzIPN, structure in **Figure 15**) was controlled, providing polymers with 95% initiation efficiency and 90% conversion in 3 h in the presence of 15 ppm of catalyst.[247]

All investigated POZ, PTZ, and DHP-catalyzed systems were involved in an oxidative quenching cycle that did not require a sacrificial electron donor, while fluorescein was reported as a metal-free catalyst for photoATRP of MMA in the presence of trimethylamine as a sacrificial electron donor.[248] Excited fluorescein activated an alkyl bromide and generated a propagating radical in a reductive quenching cycle (**Figure 19**). After photoexitation an excited fluorescein was formed and then quenched by excess trimethylamine acting as the electron donor, providing the fluorescein radical anion and an amine radical cation. The fluorescein radical anion had a sufficiently negative reduction potential to reduce the alkyl bromide, generating the propagating radicals. On the other hand, the trialkylamine radical cation oxidized the bromide anion to bromine radical. The bromine radical could react with the propagating radical in the deactivation process, or with itself to generate bromine molecule that deactivated the carbon radical. The deactivation process also competed with side reactions such as bromine radical initiated polymerization, leading to an inefficient deactivation process resulting in formation of polymers with much higher molecular weight and broad distributions. The fluorescein-catalyzed photoATRP was a less controlled process compared to metal-free ATRP catalyzed by PTZ or DHP, due to limitations in initiation and deactivation. Other photoredox catalysts in the reductive quenching mechanism were also investigated, including Eosin Y,[249] Erythrosin B,[250, 251] camphorquinone, and thioxanthone.[252]

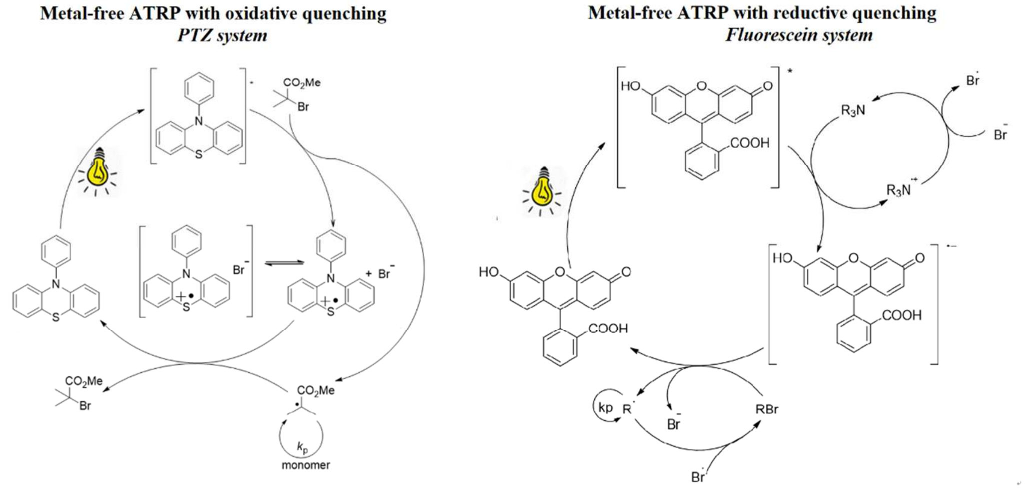

Figure 19. Proposed mechanism for metal-free ATRP with oxidative quenching (PTZ system) and reductive quenching (fluorescein system).

3.5 Applications

Multiblock copolymers. Cu-based photoATRP is a versatile RDRP method with a high polymerization rate and high retention of chain-end functionality that can be carried out under mild conditions, which allows synthesizing sequence-controlled multiblock copolymers. For example, a decablock copolymer with a molecular weight of 8,500 and low dispersity (1.16) was prepared using $CuBr_2/Me_6TREN$-mediated photoATRP.[171] The preparation of multiblock polyacrylates with segments targeting different degrees of polymerization (DP = 3, 10, 25, and 100) was also investigated.[165] Targeting higher DP per block resulted in a decrease in polymerization rate as well as a loss of chain-end functionality. Additionally, a fresh solution of $CuBr_2/Me_6TREN$ in DMSO was added with each monomer addition to maintain control over the polymerization and the reaction rates. Subsequently, α,ω-telechelic multiblock copolymers were prepared using bifunctional initiators under Cu-based photoATRP conditions.[159]

Sequence-defined polymerization. Cu-based photoATRP was also extended to sequence-defined polymerizations via single unit monomer insertions (SUMI).[253, 254] A series of monodisperse sequence-defined acrylate oligomers of up to 5 monomer units was synthesized. To avoid radical-radical termination, monomer conversion was carefully followed by online Fourier transform infrared (FTIR) spectroscopy. After monomer conversion had reached 80-90%, the reaction mixtures were purified by flash chromatography to provide the desired SUMI oligomers.

Flow chemistry. According to the Beer-Lambert law, one of the limitations of photoreactions is low illumination efficiency in the reaction mixture. This problem was resolved by using continuous flow reactors which have significant advantages such as scalability and more efficient heat release.[255, 256] PhotoATRP of MA and BA was reported with $CuBr_2/Me_6TREN$ in DMSO in a continuous flow reactor.[173] The polymerization maintained a good control with a polymerization rate 4 times faster than the rate observed in a small scale batch reaction, because of very efficient illumination. Excellent chain-end group fidelity was determined by both ESI-MS and chain extension. MMA was also polymerized in a flow reactor under Cu-mediated photoATRP conditions with PMDETA as ligand, resulting in a polymerization rate that was 7 times faster than in a batch operation. PhotoATRP based on Ir and metal-free systems were also developed under continuous flow, which showed similar process advantages.[257, 258]

Surface-initiated (SI)-ATRP. Photoreactions are excellent tools for modification of surfaces because of their ability to provide spatial and temporal control. Spatial control in photoATRP could be used to directly make specific patterns by forming polymer brushes on selected areas of the surface. Retention of high chain-end fidelity could also be used to grow block copolymer on surfaces by photoATRP.

The first copper-mediated surface-initiated photoATRP used $CuCl_2$/bpy as catalyst and TiO_2 as photosensitizer.[143] Cu-based photoATRP without photosensitizer was also applied to SI-ATRP of MMA from silicon wafers.[158] This method was also used to graft acrylates from cellulose[162] and silicon substrates.[259] A $CuBr_2$/Me_6TREN-catalyzed photoATRP in DMSO was used to graft (meth)acrylates under UV light (360 nm, 36 W) with air cooling.[259, 260] The film thickness was proportional to the irradiation time. This system used only ppm level of catalyst, even as low as 100 part per billion (ppb) concentration of copper catalyst. At such low concentration of catalyst, deactivation is typically slow so that an uncontrolled free radical polymerization could be involved.

In addition to the Cu-based photoATRP, Fe photoATRP systems[193] were also reported to be successful for surface initiated polymerizations. Pentafluoropropyl acrylate was grafted from surfaces using iron-based photoATRP.[193] Spatially resolved patterns were formed using photomasks, and preparation of a film of block copolymer was used to demonstrate the "living" nature of the procedure.

An Ir-mediated photoATRP of MMA from silicon substrates was successfully carried out from a self-assembled monolayer (SAM) of α-bromoisobutyrate (BiB)-based ATRP initiator (**Figure 20**).[261] MMA, OEGMA, and various fluorinated methacrylates were polymerized, providing polymer films with thicknesses ranging from 60 to 120 nm.[261, 262] Linear relationships between film thickness and both irradiation time and light intensity were reported. This, in addition to successful chain extension, indicated that good control was attained with this process. 3D architectures on the surface were directly obtained using a photomask with different optical densities.

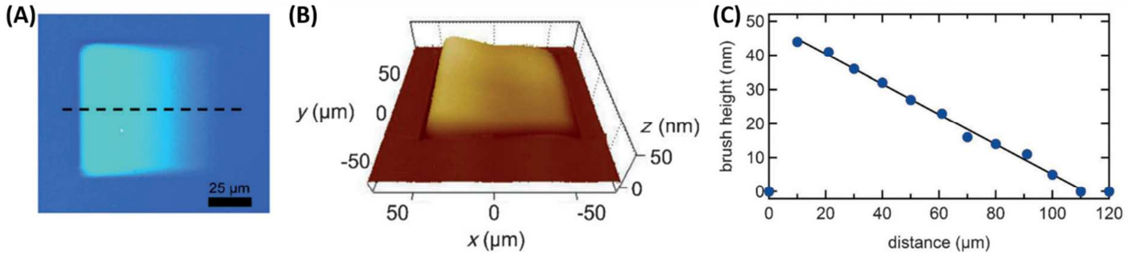

Figure 20. (A) Optical micrograph and (B) AFM image of nanoscale-inclined plane formed from polymer brushes upon light exposure through a shadow mask with optical density gradient. (C) Height

along dashed line across feature as shown in (A). (Reproduced from Ref. [261], copyright 2013 with permission from Wiley.)

Metal-free photoATRP was also extended to the fabrication of surface-tethered films using phenothiazine-based photoredox catalysts generating well-defined polymer brushes from nanoparticles and from flat or curved surfaces.[263] Upon irradiation, with either compact fluorescent lamps or natural sunlight, different architectures such as single-layer patterns, gradient structures, and block copolymers were obtained. In a follow up study, tetherable initiators based on 2-bromo-2-phenylacetate were synthesized and used for surface modification of silica nanoparticles providing superior initiation properties and higher grafting density compared to a BiB-modified surface in metal-free SI-ATRP catalyzed by PTZ.[264] The effect of the spacer length within the tetherable initiator was investigated for Cu-catalyzed and PTZ-catalyzed photoinduced metal-free SI-ATRP.[265]

Bioconjugation and autoATRP. A commercial DNA synthesizer was reconfigured to carry out copper-catalyzed photoATRP in an automated fashion, a procedure termed autoATRP. Well-defined homopolymers, diblock copolymers, and DNA-polymer hybrids were prepared.[266] PhotoATRP with excess ligands does not require any additional photoinitiator or photosensitizer, and provides a clean polymerization with oxygen tolerance under mild reaction conditions. The procedure was especially suitable for preparation of a range of different bioconjugates.

Gels. Structurally tailored and engineered macromolecular gels (STEM gels) have been synthesized by free radical copolymerization of monomer, crosslinker, and a photoactive inimer based on Irgacure 2959. The gel network with latent Irgacure photoactive initiating sites allowed for spatial post-modification after infiltration of a second monomer in the "parent" network.[267] This strategy of "living additive manufacturing" provided complex and diversely functionalized "daughter" gels by spatiotemporal modification of the "parent" gels, which were infiltrated with a second monomer and irradiated to trigger a conventional radical polymerization.[268]

Recently, this concept has been extended to CRP methods,[269] which produced a more homogeneous network and had better control over the STEM gel modifications than conventional radical polymerization. The "parent" networks were prepared by RAFT polymerization, and the incorporation of an ATRP initiator monomer (inimer) during the RAFT polymeirzation allowed for successive orthogonal modifications (**Figure 21**). The resulting STEM gels were infiltrated with a second monomer, which was grafted from the inimer sites by photoATRP. Depending on the choice of this second monomer for the side chains, several different properties were varied: hydrophobic STEM gels were converted to hydrophilic gels and temperature and pH response were introduced. In addition, by using a photo-mask, the pristine parent networks were spatially differentiated into single-piece amphiphilic and hard/soft materials without the need for a gluing agent. For example, a soft poly(2-(2-methoxyethoxy)ethyl methacrylate) STEM gel was modified with PMMA side chains to create hard/soft regions. After the introduction of side chains, the Young's modulus (E) increased by an order of magnitude.

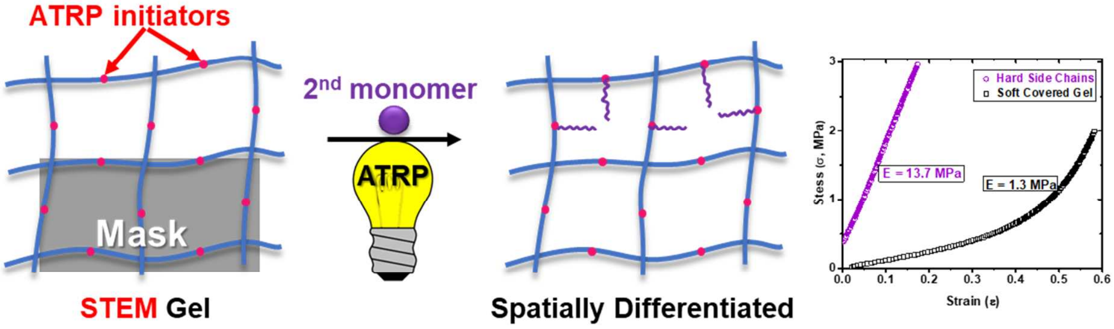

Figure 21. Post-synthesis modification of STEM gels by infiltrating a second monomer (purple) and an ATRP catalyst, and subsequent grafting-from by photo ATRP with possible spatial control. After half of the soft parent STEM gel was grafted with high-T_g PMMA side chains, stress (σ, MPa) vs. strain (ε) traces were acquired in compressibility tests. The open black square symbols (□) correspond to the unmodified half and the purple open symbols correspond to the modified half (○). The slopes of linear regime, which correspond to the values of Young's modulus E (MPa), are shown in boxes located next to respective curves.

The photocatalyst 10-phenylphenothiazine was covalently attached to a thermal responsive gel by modification of the side rings of the organic catalyst (Gel-PTZ). This embedded catalytic system provided polymerization control from within the network by application of multiple external stimuli such as light and heat, with the ability to start and stop the polymerization with an "AND" logic (**Figure 22**).[270] The catalyst activity could be tuned by both switching the light "ON"/"OFF" and by changing temperature to “HIGH”/”LOW” values, which caused collapse or expansion of the polymer network.

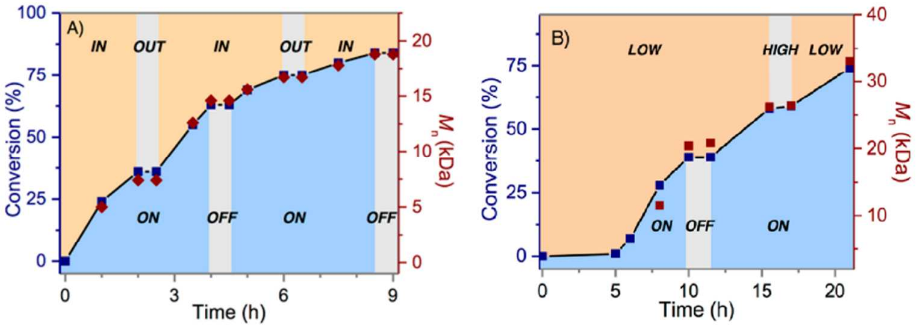

Figure 22. A) “AND” Logic-CRP enabled by Gel-PTZ catalyst. Light “ON”/“OFF” and catalyst “IN”/“OUT” controlled polymerization. B) “AND” Logic-CRP with Light “ON”/“OFF” and Temperature “LOW”/“HIGH” enabled by Gel-PTZ catalyst. (Reproduced from [270], copyright 2017 with permission from the American Chemical Society.)

IV. MechanoATRP

Ultrasound is the latest developed method to introduce electrons and regenerate the activator complex in an ATRP system. Inspired by ultrasound-induced redox reactions at the interface of a piezoelectric material occurring in water splitting[271] and charge separation in electrochemical cells[272], a mechanically controlled ATRP (mechanoATRP) was conducted with ultrasound in the presence of piezoelectric $BaTiO_3$ nanoparticles.[53] This process is different from the conventional ultrasound-mediated radical polymerizations that utilized force-induced cleavage of labile bonds,[273] as this method is based on piezochemically initiated controlled radical polymerization that converted mechanical energy into electrons at the interface of the piezoelectric material via charge separation.

Similar to other stimuli-mediated electron transfer procedures, such as photoinduced electron transfer (PET), mechanoATRP involves a mechano-induced electron transfer (MET) process which transduces a mechanical stimulus to an electrical signal.[274] $BaTiO_3$[53] and ZnO nanoparticles[54] were used as the transducers, while Cu(II) complexes were used as the catalyst in mechanoATRP. Under ultrasonic agitation as mechanical stimulus, electron transfer from piezoelectric particles to Cu(II) precursor generated Cu(I)-based species to activate the alkyl halide. Continuous growth of the polymer chain was achieved by continuous application of ultrasound. The mechanical force was used to control the length of a growing polymer chain.[54]

Several factors regulated the mechanoATRP process. The first one was the dielectric constants (ε) of the transducers. A larger dielectric constant provided a more efficient electron transfer to the Cu catalysts.[55] The second factor was the crystal structure and particle size of the transducers. For example, the tetragonal $BaTiO_3$ crystals are highly distorted and showed a stronger piezoelectric effect than the cubic phase $BaTiO_3$ nanoparticles (NPs). The smaller NPs gave a higher mechanoelectric conversion because of a larger surface/interface effect and higher specific area.[55] The third factor was the loading of transducer particles. Higher loading resulted in a faster polymerization rate, which indicated a higher concentration of radicals. [53] The fourth factor was the addition of a surface modifier. In order to increase electron transfer efficiency between transducers and electron acceptors in this heterogeneous system, a series of solubilizers and surface modifiers were used to stabilize the transducer nanoparticles and keep them uniformly dispersed.[55]

Despite $BaTiO_3$ having a much larger piezoelectric coefficient that ZnO, the latter was a more efficient reducing agent under ultrasonication due to the smaller size of the ZnO particles and due to a strong interaction with Cu(II) complexes that enhanced the local catalyst concentration on the particle surface.

The mechanical forces (i.e. ultrasound) used in mechanoATRP had deeper penetration into the reaction medium than light, which had limited access into the bulk of monomer and solvents in a stirred flask. Moreover, mechanoATRP systems were not affected by light-scattering in gels or heterogeneous systems.[55] MechanoATRP was also used as a switchable controlled radical polymerization technique, in which the electron transfer process was mediated through the application or removal of the external stimulus. This strategy enabled mechanoATRP with a spatial and temporal control over reaction kinetics, composition, architecture, and functionality through stopping and restarting the driving force.[54] Monomer conversion was negligible in the absence of sonication, while the polymer chain length continuously grew after re-exposure to the mechanical force (**Figure 23**). Additionally, polymers prepared by mechanoATRP retained all properties of materials made by conventional ATRP, such as low dispersity, precisely controlled molecular weights, and high retention of chain-end functionality.

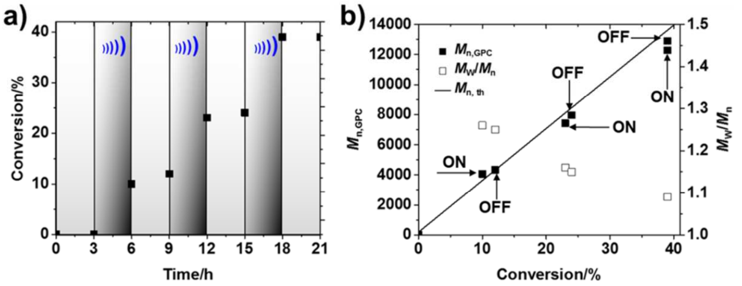

Figure 23. Temporal control in mechanoATRP with a low loading of ZnO via switching on/off the ultrasound bath. a) Kinetics and b) molecular weight and dispersity of polymers. Reaction conditions $[MA]/[EBiB]/[CuBr_2]/[TPMA] = 400/1/0.03/0.18$, 0.15 wt% ZnO (18 nm), in 50% (v/v) DMSO. (Reproduced from [54], copyright 2017 with permission from the American Chemical Society.)

Several activation pathways for ZnO-catalyzed mechanoATRP were considered and are summarized in **Scheme 8**.[54] The predominant role of ZnO was to provide electrons to reduce Cu(II) under sonication. A second possibility was the formation of radicals from monomer/solvent by cavitation, but this was a slow process. Direct reduction of alkyl halide by ZnO and homolytic cleavage of TPMA/Cu(II)-halogen bond under sonication were both excluded as potential activation procedures by experimental evidence.

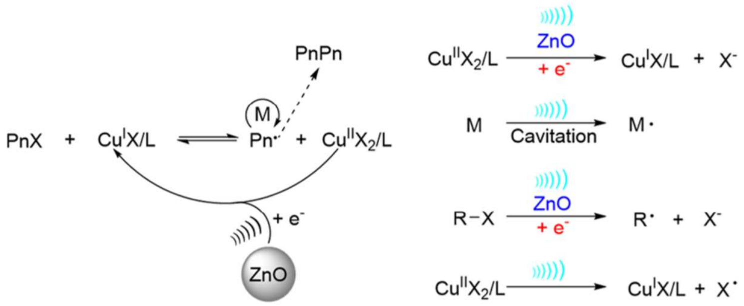

Scheme 8. Proposed mechanism of mechanoATRP and pathways of activator (re)generation. (Reproduced from [54], copyright 2017 with permission from the American Chemical Society.)

An ultrasonication-induced ATRP (SonoATRP) in aqueous media was recently developed to polymerize OEOMA and 2-hydroxyethyl acrylate (HEA) using ppm level of copper as catalyst and TPMA as ligand in the absence of any piezoelectric materials (**Scheme 9**).[56] SonoATRP proceeded with a different mechanism than mechanoATRP, and did not require the presence of piezoelectric materials. An ultrasonic wave propagated through water and generated hydroxyl radicals via acoustic cavitation, which initiated polymerization of vinyl monomers thereby forming carbon radicals. A similar activation mechanism was applied to induce RAFT polymerization in aqueous media.[275]

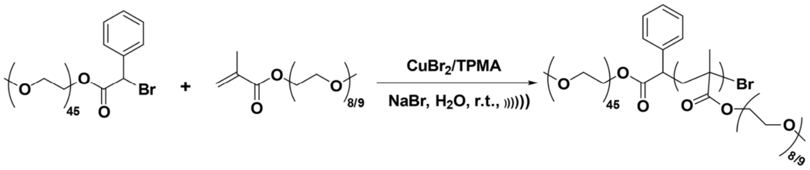

Scheme 9. The reaction scheme for aqueous sono-ATRP of OEOMA500.

V. Chemical control

5.1 ARGET ATRP

In addition to physical stimuli, chemical stimuli could also modulate an ATRP process in the presence of a very low concentration of catalyst. Various chemical reducing reagents can continuously regenerate the activators from the deactivators through electron transfer. [30, 31, 276-280] Thus, activators regenerated by electron transfer (ARGET) ATRP was applied to significantly decrease catalyst concentration to 10 ~ 100 ppm, without losing control of the polymerization.[281-283] Moreover, the presence of excess of reducing reagent not only regenerated activators, but also provided tolerance to oxygen and other radical inhibitors, making the polymerization simpler to operate.[282] Various organic chemical reducing agents were reported to successfully regulate the polymerization process, such as ascorbic acid,[280] sugars,[279] derivatives of hydrazine, and phenol, [31] as well as inorganic chemicals including tin(II) complexes [276, 277, 279] and metals.[281] In addition, some monomers or nitrogen-based ligands also acted as reducing agents.[284, 285]

Recently, ionic liquids[286] and water[287] were used to synthesize bio-relevant polymers. ARGET ATRP of OEOMA was successfully implemented by slow addition of ascorbic acid in aqueous media in the presence of 100 ppm of catalyst. [288] The polymerization was stopped and (re)started by alternating the feeding of ascorbic acid, similar to current in *e*ATRP or light in photoATRP. The polymerization was faster during the feeding periods, but some monomer conversion was observed without feeding ascorbic acid during the "off" periods (**Figure 24**). This temporal control was incomplete due to residual Cu(I) and ascorbic acid, which still regenerated activators.

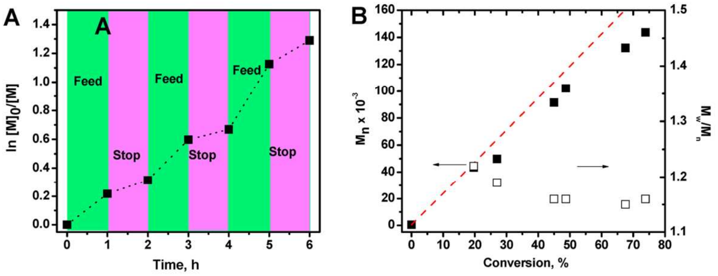

Figure 24. Effects of the feeding of ascorbic acid in ARGET ATRP of OEOMA in water. A) Kinetics and B) molecular weight and dispersity of polymers. Reaction conditions:

[OEOMA]/[RX]/[$CuBr_2$]/[TPMA] = 500/1/0.15/1.2, [OEOMA] = 0.5 M. (Reproduced from [288], copyright 2012 with permission from the American Chemical Society.)

Chemically controlled ARGET ATRP enabled polymerization with a low catalyst concentration, providing high retention of end-group, and tolerance to limited amounts of air. [30, 282] Moreover, the procedure started with oxidatively stable Cu(II) deactivators which were easier to handle and less expensive. The benefits of this robust polymerization technique made significant contributions to synthesize various complex and precisely controlled polymeric architectures, such as blocks, [289, 290] stars, [291, 292] and bottlebrush copolymers, [293-295] as well as surface modified composites [296, 297] and protein-polymer bio-conjugates [298, 299] with low concentrations of catalyst.

5.2 SARA ATRP

In addition to the chemical reducing agents employed in ARGET ATRP, zerovalent metals can be used as reducing agents for the reduction of stable high-oxidation-state deactivators. Zerovalent metals also directly activate the dormant chain end, acting as supplemental activators [300]. Originally, the addition of copper powder to either Cu(I) or Cu(II) complexes in an ATRP could significantly increase the rate of the polymerization of styrene and (meth)acrylates.[301] It was demonstrated that the normal ATRP process could be triggered with different forms (powders, wires, turnings, mesh, etc.)[302] of Cu(0) or Fe(0) in the presence of limited amount of air. [300, 303] The addition of zerovalent metals not only reduced the deactivators (higher oxidation state species) formed due to the persistent radical effect, but also directly activated the chain-end of alkyl halides.[38, 304] However, the main activation process (>99%) relies on Cu(I) activators. Hence, this technique was named supplemental activator and reducing agent (SARA) ATRP.[33, 39, 305, 306]

Cu(0) is typically used in SARA ATRP. Cu(0) comproportionates with the Cu(II) deactivators, which increases the concentration of Cu(I) activators. The Cu(I) complexes are highly reactive and rapidly react with the alkyl halides, while their disproportionation to Cu(0) and Cu(II) is suppressed, as confirmed by several experimental results and kinetic simulations.[35-37] Supplemental activators with low toxicity include zerovalent metals such as Fe(0),[40, 307] Mn(0), [40] Zn(0), [40] and Ag(0),[304,308] as well as inorganic sulfites such as sodium dithionite ($Na_2S_2O_4$), [309] sodium metabisulfite ($Na_2S_2O_5$),[309] and sodium bisulfite ($NaHSO_3$).[32] Moreover, the versatile SARA ATRP procedure was also implemented in environmentally friendly solvents, such as water[38] and ionic liquids,[310, 311] showing a much increased polymerization rate due to increased K_{ATRP} and increased solubility of dithionite salts.[312]

SARA agents in a solid form, such as metals, could be removed from the system through lifting out from the reaction mixture, even with an external magnetic field, [35] and could be reused several times. For example, a single piece of silver wire was used five times in the polymerization of BA without any treatments prior to reuse.[304] The rate of polymerization did not significantly change after each cycle, and a high degree of control was obtained in all polymerizations (**Figure 25**).

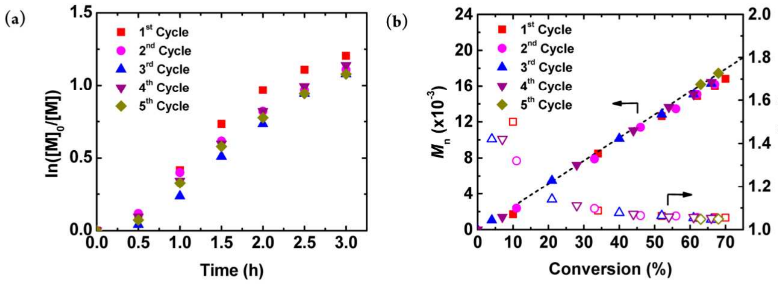

Figure 25. (a) Kinetics and (b) evolution of M_n and M_w/M_n with conversion in the ATRP of BA with the same silver wire in five sequential reactions. Reaction conditions: $[BA]_0$:$[EBiB]_0$:$[CuBr_2]_0$:$[TPMA]_0$ = 200:1:0.04:0.08 with $[BA]_0$ = 3.49 M in DMF at 50 °C, in the presence of 5 cm Ag^0 wire (d = 2 mm, SA = 3.2 cm^2 ; V_{tot} = 10 mL). (Reproduced from [304], copyright 2015 with permission from the American Chemical Society.)

This method is useful for post-modification procedures and for the synthesis of multiblock copolymers, also in bio-compatible environments;[102,313,314] for example, molecular bottlebrush polymers were prepared by SARA ATRP in the presence of 2.5 cm Cu wire and 50 ppm Cu-based catalyst at 30 °C.[315]

SARA surface-initiated ATRP. SARA-ATRP was also employed for surface initiated polymerization.[316] Three cationic coatings including (3-acrylamidopropyl) trimethylammonium chloride (AMPTMA), quaternized poly(ethylenimine) methacrylate (Q-PEI-MA) and poly(ethylene glycol) dimethacrylate (PEGDMA) were successfully coated on a compatible catheter surface via SARA SI-ATRP which presented good bactericidal killing results *in vivo*.[317]

Surface-initiated ATRP catalyzed by Cu^0 plates was recently reported as a fast and versatile tool to fabricate structured polymer brushes on flat surfaces.[318] In a typical setup, a Cu plate is positioned at a distance of ~ 0.5 mm from a surface functionalized with ATRP initiator. In the presence of ligand, copper species cleaved from the Cu^0 surface could activate the neighboring initiator surface and very quickly trigger the formation of a uniform layer of polymer brushes. The procedure was compatible with large substrates.[319] Moreover, the accessibility of the reaction setup enabled the synthesis of polymer brush gradients simply by tilting the Cu plate above the initiating surface, thus locally altering the concentration of catalyst that reached the surface-immobilized initiators/dormant species.[320] It is important to note that in these experiments the Cu(0) surface acted only a source of Cu(I) catalyst, and not as a supplemental activator, due to the physical separation between the Cu(0) plate and the initiator-functionalized surface.

Temporal control in ATRP using zerovalent metals. Recently, temporal control in ATRP was extended to SARA ATRP in the presence of zerovalent metals such as Cu^0 or Ag^0 with a simple but effective experimental procedure.[321] The metal wire was inserted into the reaction medium to start the reaction, and lifted out of the solution to switch the reaction off. Inserting a wire in the solution triggered the polymerization by (re)generation of Cu(I)/L activator species, whereas lifting the wire out of the solution stopped regeneration of the activators. While the wire was lifted out of the solution, the residual Cu(I) catalyst was consumed by termination of radicals, stopping the reaction. However, efficiency of this procedure depends on the concentration of Cu and ligand species, and also on the ATRP equilibrium constant (i.e. fraction of Cu(I) among all soluble Cu species). For example, using the most active ligands such as Me_6TREN or $TPMA^*3$ the reaction proceeded smoothly in the presence of Cu(0) wire, and it essentially stopped after lifting the wire out from the reaction mixture (**Figure 26A**). The large K_{ATRP} values associated with these ligands shift the equilibrium towards Cu(II) species (i.e., less Cu(I)), and hence the reaction stops quicker. With less active complexes (TPMA, PMDETA) this effect is less pronounced due to a lower equilibrium constant and more Cu(I)/L available even without Cu(0) wire.

In SARA ATRP with Cu wire, with enough ligand, the total concentration of soluble Cu increases continuously throughout the reaction, as a result of supplemental activation and activator regeneration via comproportionation. However, in SARA ATRP with Ag wire, a constant concentration of Cu is maintained (**Figure 26B**), since supplemental activation is negligible and only reduction of deactivators occurs. Interestingly, the reaction was slower with the most active complex (Cu/TPMA^{*3} compared to Cu/Me$_6$TREN) due to slower reduction of the most active species that has a more negative redox potential.

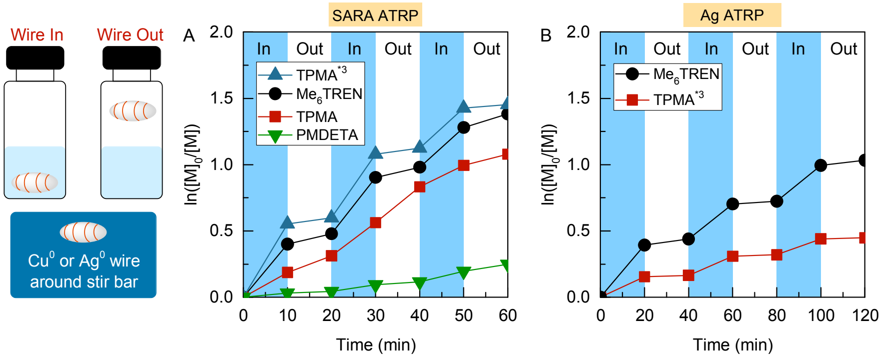

Figure 26. Kinetics of temporal control in (A) SARA ATRP with Cu^0 wire and (B) ATRP in the presence of Ag^0 wire with different ligands. Reaction conditions: [MA]/[EBiB]/[CuBr$_2$]/[L]: 200/1/0.05/0.15 (L: Me$_6$TREN, PMDETA, TPMA, or TPMA^{*3}) in 50 vol% DMSO, at 30 °C; Cu^0 wire length: 5 cm, diameter: 0.5 mm; Ag^0 wire length: 5 cm, diameter: 2.0 mm.

VI. Thermal control

6.1 ICAR ATRP

Perhaps the simplest and most widely used and external modulation is through thermal control, which allows for "on" and "off" switching by using instrumentation available in every laboratory. Different from the ARGET ATRP technique that requires chemical reducing agents to continuously regenerate activators *in situ*, an ICAR ATRP utilizes conventional radical initiators to slowly generate radicals and thus diminish the accumulation of deactivators the system.[31] Initially, it was determined that the self-initiation process in the polymerization of Sty generated radicals that reduced the concentration of the accumulated deactivator. It was then proposed that addition of small amount of a radical initiator to other monomers could also initiate the polymerization and yield well-defined polymers.

Unlike the reverse ATRP and simultaneous reverse and normal initiation (SR&NI) ATRP that utilized large amounts of radical initiators and high temperature to rapidly decompose the initiator, ICAR ATRP relied on a constant slow release of radicals at lower temperature to maintain the rate of polymerization. [322] In reverse and SR&NI ATRP, high concentration of radicals led to bimolecular termination and initiation of new polymer chains; conversely, slow generation of radicals in ICAR ATRP continuously reduced the deactivators to activators and afforded polymerization with better control on molecular weight and low dispersity. AIBN with 10 h half lifetime at 65 ^{o}C and water-soluble 2,2`-azobis[2-(2-imidazolin-2-yl)propane] dihydrochloride (VA-044) with 10 h half lifetime at 44 ^{o}C were commonly used as the thermal initiators. [323, 324] ICAR ATRP was usually conducted with Cu [323, 325-327] or Fe-based catalysts [324, 328, 329] in a range of solvents, including ionic liquids, [330] poly(ethylene glycol) [331] and water.[323]

ICAR ATRP maintained the advantages of ARGET ATRP with low concentrations of catalyst, tolerance to limited amount of air, and high end-group retention. It was used to synthesize various advanced materials such as soft nanomaterials, [332-334] nanotubes, [335] hybrid inorganic/organic materials, [336, 337] biofluorescent imaging agents, [338] and polymer-protein bioconjugates. [323, 339] Well-defined mesoporous carbon/poly(glycidyl methacrylate) (PGMA) composites were prepared by surface-initiated ICAR ATRP of glycidyl methacrylate (GMA) monomer within the mesoporous carbon framework, which preserved high chain-end functionality for further modification.[336] A similar work was conducted on the surface of ordered mesoporous silica (OMS) by *in situ* growth of functional PGMA brushes on the OMS surface, which was post-modified for lithium isotope separation.[337] Additionally, ICAR ATRP could be implemented in aqueous systems to polymerize hydrophilic $OEOA_{480}$ that could be directly used to prepare bioconjugates by growing the macromolecules on a bovine serum albumin (BSA) protein modified with initiators.[323]

6.2 "Breathing" ATRP

Glucose oxidase (GOx) was previously used to scavenge oxygen in the presence of glucose during free radical and RAFT polymerizations.[340-343] The same enzyme-assisted deoxygenating strategy was applied to aqueous ICAR ATRP using VA-044 as radical initiator in the open air.[344] The polymerization of $OEOMA_{500}$ with HEBiB as the ATRP initiator was conducted in phosphate buffer saline (PBS) at 45 °C, yielding polymers with low dispersity but MW four timers lower than the theoretical values. This discrepancy suggested that hydrogen peroxide, formed from the reaction between glucose, GOx, and oxygen, continuously generated new chains through a Fenton-like reaction with Cu(I) to yield initiating hydroxyl radicals, which strongly diminished the possibility to control MW. Therefore, sodium pyruvate was added to the reaction to eliminate this reactive oxygen species. Sodium pyruvate consumed the hydrogen peroxide forming carbon dioxide, acetate ions, and water, which allowed the polymerization in the open air without formation of new chains. These conditions yielded polymers with predictable MW and low dispersity at almost complete conversion in less than 2 hours. The temporal on/off control was investigated using thermoregulation between heating to 45 °C and cooling to 0 °C (**Figure 27**). At 45 °C, VA-044 decomposed to radical initiating the polymerization, while at 0 °C the decomposition was stopped to quench the polymerization. Using this thermoregulation strategy, the temporal control of breathing ATRP was achieved.

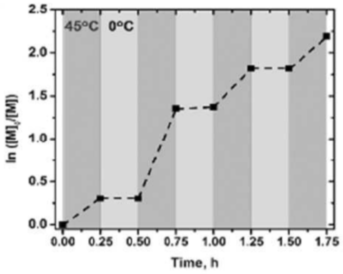

Figure 27. Kinetic plots of temporal control of on/off study under different temperatures (45 °C and 0 °C), conditions: M = $OEOMA_{500}$, [M] = 10 vol % in PBS, [NaBr] = 100 mm, [glucose] = 200 mm, [GOx] = 2 μm, [sodium pyruvate] = 100 mm. (Reproduced from [344], copyright 2018 with permission from the Wiley.)

6.3 *Ultimate ATRP^{SM}*

A process called *Ultimate ATRP^{SM}* was developed to scale-up the ATRP process.[345] This method precisely controls the activator/deactivator ratio during ATRP through feeding radical initiators at a controlled rate at a temperature high enough to provide a very short half-lifetime (a few minutes) for the added initiator. In classic ICAR ATRP, the entire amount of radical initiator was initially added, and during the reaction the amount of decomposed radical initiator gradually decreased (**Figure 28**). However, in the *Ultimate ATRP^{SM}* process, a low concentration of radical initiator was kept at a constant level during the feeding time.

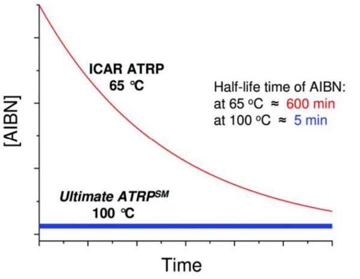

Figure 28. Theoretical concentration of AIBN during the polymerization in ICAR ATRP and in the *Ultimate ATRP^{SM}* process. (Reproduced from [345], copyright 2012 with permission from the American Chemical Society.)

The polymerization of Sty via the *Ultimate ATRP^{SM}* process was conducted using 50 ppm of $CuBr_2$ and small excess of TPMA ligand. A toluene solution of AIBN was fed at the constant rate 0.008 equiv. (ratio to ATRP initiator) per hour. The reaction was efficiently stopped after 9 h by interrupting feeding and heating (**Figure 29**). Polymerization was restarted at 110 °C using the same feed rate of the AIBN solution. The temperature profile indicated good heat transfer. This technique featured temporal control that was especially useful for industrial scale applications such as checking product quality and controlling exothermic reactions.

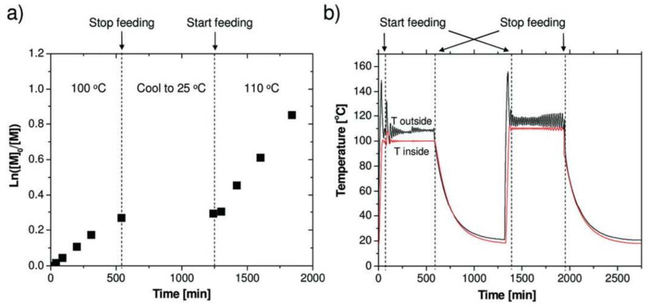

Figure 29. a) Kinetic plot and b) temperature profile during the polymerization of styrene using the *Ultimate ATRP*^{SM} process. Conditions: Sty/RX/$CuBr_2$/TPMA/AIBN = 1000/1/0.05/0.15/fed; bulk at 100-110 °C; 50 ppm of Cu; feeding rate = 3.33 mL/h (0.008 eq. of AIBN vs. diethyl 2-bromo-2-methylmalonate initiator in 1 h). (Reproduced from [345], copyright 2012 with permission from the American Chemical Society.)

VII. Summary and outlook

External control in ATRP provides pre-designed polymeric materials under spatiotemporal control while employing very low concentrations of catalyst. To date, electrochemical and photochemical mediated processes have been the most widely studied for external regulation. The next generation of photoATRP should target softer irradiation sources such as low light intensity and red/near-infrared light wavelengths.[346] This could potentially provide the possibility of polymerization in various medical applications (plausibly *in vivo*). Moreover, smart catalysts with more than one active catalytic center could be designed to give selective reactivity under different light irradiation or applied electrochemical potential conditions.[347, 348] PhotoATRP also provides the possibility of 3D printing with high resolution. Other stimuli such as chemical and thermal control are intrinsic parts of ARGET and ICAR ATRP; however, spatiotemporal control in these systems have not been yet tested. Spatial control in mechanoATRP should also be explored. Surface-initiated ATRP in the presence of Cu^0 should be exploited as a facile platform to grow structured polymer surfaces.

All of the switchable ATRP systems have been examined for the straightforward turning on or off the polymerization. However, a more sophisticated modulation of catalyst reactivity *in situ* is still underdeveloped, such as selective polymerization of specific monomers. Future efforts should be directed toward achieving intelligent control with multiple stimuli, potentially with stimuli that can complement or negate/block each other. The concept of logical gate, widely adopted in electronics, could be subsequently developed to achieve “AND” conjunction and “OR” disjunction, among others. Perhaps the simplest example for “OR” logical gate is using AIBN in PhICAR process, in which either photochemical or thermal conditions would induce polymerization. Combining different types of stimuli will provide a synergistic advanced system that resembles self-regulatory and biological processes. Externally controlled ATRP represents a useful alternative to conventional ATRP and is expected to achieve more challenging targets that are currently impossible to accomplish.

Abbreviations

4CzIPN	1,2,3,5-tetrakis(carbazol-9-yl)-4,6-dicyanobenzene
AA	acrylic acid
AIBN	2,2'-azobis(2-methylpropionitrile)
AMPTMA	(3-acrylamidopropyl) trimethylammonium chloride
AN	acrylonitrile
ARGET	activators regeneration by electron transfer
ATRP	atom transfer radical polymerization
BA	butyl acrylate
BMA	butyl methacrylate
bmim	1-butyl-3-methyl-imidazolium
BnMA	benzyl methacrylate
BPE	bipolar electrode
BPMEA	*N*,*N*-bis(2-pyridylmethyl)-2-hydroxyethylamine
BPMODA*	bis[2-(4-methoxy-3,5-dimethyl)-pyridylmethyl]octadecylamine
BPN	2-bromopropionitrile
BPO	benzoyl peroxide
bpy	bipyridyl
$BrPhN_2$	4-bromobenzenediazonium
BSA	bovine serum albumin
btp	2-(2`-benzothienyl)pyridine
cHE	catalytic halogen exchange
CPAD	4-cyano-4-(phenylcarbonothioylthio)pentanoic acid
CRP	controlled radical polymerization
CTAs	chain transfer agents
CV	cyclic voltammetry
DHP	dihydrophenazines
DMA	dimethylacetamide
DMAEMA	dimethyl amine methacrylate
DMF	dimethylformamide
DMSO	dimethyl sulfoxide
dppm	bis(diphenylphosphino)methane
DP	degrees of polymerization

DT	degenerative transfer
EA	ethyl acrylate
EBiB	ethyl α-bromoisobutyrate
EBPA	ethyl α-bromophenylacetate
EClPA	ethyl α-chlorophenylacetate
ESI-MS	electrospray-ionization mass spectrometry
Et_4NCl	tetraethylammonium chloride
FTIR	Fourier transform infrared
GMA	glycidyl methacrylate
GOx	glucose oxidase
HE	halogen exchange
HEA	hydroxyethyl acrylate
HMTETA	*N*,*N*,*N*`,*N*``,*N*```,*N*```-hexamethyltriethylenetetramine
ICAR	initiators for continuous activator regeneration
ISET	inner sphere electron transfer
LED	light-emitting diode
LFP	laser flash photolysis
MAA	methacrylic acid
MALDI-TOF	matrix-assisted laser desorption/ ionization time of flight
MBiB	methyl 2-bromoisobutyrate
Me_6TREN	tris[2-(dimethylamino)ethyl]amine
MeCN	acetonitrile
Me-PTZ	10-methylphenothiazine
MET	mechano-induced electron transfer
MF-ATRP	metal-free ATRP
MMA	methyl methacrylate
MOF	metal organic framework
NIR	near infrared
O-ATRP	organocatalyzed ATRP
OEGA	oligo(ethylene glycol) methyl ether acrylate
OEGMA	oligo(ethylene glycol) methacrylate
OEOA	oligo(ethylene oxide) methyl ether acrylate
OEOMA	oligo(ethylene oxide) methyl ether methacrylate
OMS	ordered mesoporous silica
OSET	outer sphere electron transfer

PAN	poly(acrylonitrile)
PBA	poly(butyl acrylate)
PBS	phosphatebuffer saline
PEG	polyethylene glycol
PEGDMA	poly(ethylene glycol dimethacrylate)
PET	photoinduced electron transfer
PGMA	poly(glycidyl methacrylate)
Ph-benzoPTZ	phenyl benzo[*b*]phenothiazine
Phen	1,10-phenanthroline
PhICAR	photoICAR
Ph-PTZ	10-phenylphenothiazine
PLP	pulsed-laser polymerization
PMA	poly(methyl acrylate)
PMDETA	*N*,*N*,*N*',*N*'',*N*''-Pentamethyldiethylenetriamine
PMMA	poly(methyl methacrylate)
ppb	part per billion
PPh_3	triphenylphosphine
ppm	parts per million
ppy	2,2'-phenylpyridine
PTZ	phenothiazine
Q-PEI-MA	quaternized polyethylenimine methacrylate
RAFT	reversible addition-fragmentation chain transfer polymerization
RDRP	reversible-deactivation radical polymerization
RX	alkyl halides
SAM	self-assembled monolayer
SARA	supplemental activators and reducing agents
SDS	sodium dodecyl sulfate
SET-LRP	single electron transfer living radical polymerization
SFRP	stable free-radical polymerization
SI	surface-initiated
SR&NI	simultaneous reverse & normal initiation
Sty	styrene
STEM	structurally tailored and engineered macromolecular
SUMI	single unit monomer insertions
TFEMA	1,1,1-trifluoroethyl methylacrylate

tmd	2,2,6,6-tetramethyl-3,5-heptanedione
TMEDA	tetramethylethylenediamine
TPMA	tris[(2-pyridyl)-methyl]amine
TPMA*3	tris((4-methoxy-3,5-dimethylpyridin-2-yl)methyl)amine
TREN	tris(2-aminoethyl)amine
UV	ultraviolet
VA-044	2,2`-azobis[2-(2-imidazolin-2-yl)propane] dihydrochloride
Vis	visible

Acknowledgments: X.P. acknowledges the support from the National Natural Science Foundation of China (21704017). Contributions from Sajjad Dadashi-Silab and Julia Cuthbert are gratefully acknowledged. Support form NSF: DMR 1501324 and CHE 1707490 is gratefully acknowledged.

Xiangcheng Pan

Xiangcheng Pan is an associate professor and principal investigator in State Key Laboratory of Molecular Engineering of Polymers and Department of Macromolecular Science at Fudan University. In 2014, he obtained his PhD in organic chemistry from University of Pittsburgh under guidance of Prof. Dennis P. Curran. He then spent three years of postdoctoral research at the group of Krzysztof Matyjaszewski at Carnegie Mellon University working on externally controlled ATRP. In 2017, he returned to China and joined Fudan University. The research interests of his group focus on development of novel polymerization methods and radical chemistry.

Marco Fantin

Marco Fantin is a postdoctoral associate at the Matyaszewski Polymer Group. He received his Ph.D. in 2016 from University of Padova, Italy, under the guidance of Prof. A. A. Isse and Prof. A. Gennaro, at the Electrocatalysis and Applied Electrochemistry Group. He then joined the Matyjaszewski Polymer Group at Carnegie Mellon University, Pittsburgh, US. His research focuses on developing electrochemical methods to investigate and improve controlled radical polymerizations, including atom transfer radical polymerization (ATRP), reversible addition-fragmentation chain-transfer polymerization (RAFT), and polymerization in dispersed media.

Fang Yuan

Fang Yuan is a research assistant at Prof. Pan's group. She obtained her Bachelor of Science degree from Chongqing Normal University in 2014 and earned master degree from Soochow University in 2017. Her research focuses on application of radical borane chemistry in polymer synthesis.

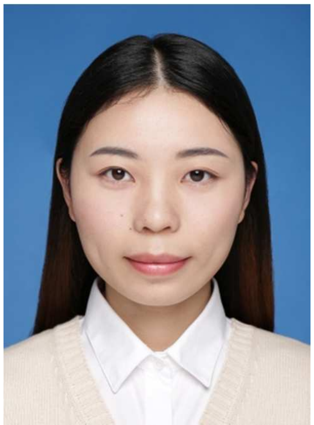

Krzysztof Matyjaszewski

Krzysztof Matyjaszewski is J.C. Warner University Professor of Natural Sciences at Carnegie Mellon University. He discovered Cu-mediated atom transfer radical polymerization, commercialized in 2004 in US, Japan and Europe. He has co-authored >1000 publications (cited >127,000 times, h-index 172, Google Scholar) and holds 59 US patents. Matyjaszewski received 2017 Franklin Medal in Chemistry, 2015 Dreyfus Prize in Chemical Sciences, 2014 National Institute of Materials Science (Japan) Award, 2011 Wolf Prize in Chemistry, 2009 Presidential Green Chemistry Challenge Award, and from the ACS:

2015 Overberger Prize, 2013 AkzoNobel North America Science Award, 2011 Hermann Mark Award, 2011 Award in Applied Polymer Science, 2002 Polymer Chemistry Award, 1995 Creative Polymer Chemistry Award. He received 10 honorary degrees and is a member of National Academy of Engineering, Polish Academy of Sciences, Russian Academy of Sciences, and National Academy of Inventors.

References

1. R. B. Grubbs and R. H. Grubbs, *Macromolecules*, 2017, **50**, 6979-6997.
2. M. Szwarc, *Nature*, 1956, **178**, 1168.
3. A. Goto and T. Fukuda, *Prog. Polym. Sci.*, 2004, **29**, 329-385.
4. W. A. Braunecker and K. Matyjaszewski, *Prog. Polym. Sci.*, 2007, **32**, 93-146.
5. K. Matyjaszewski and T. P. Davis, *Handbook of radical polymerization*, Wiley Online Library, 2002.
6. A. H. E. Müller and K. Matyjaszewski, *Controlled and Living Polymerizations*, Wiley-VCH Verlag GmbH & Co. KGaA, 2010.
7. D. Jenkins Aubrey, G. Jones Richard and G. Moad, *Pure Appl. Chem.*, 2009, **82**, 483.
8. C. J. Hawker, A. W. Bosman and E. Harth, *Chem. Rev.*, 2001, **101**, 3661-3688.
9. J. Nicolas, Y. Guillaneuf, C. Lefay, D. Bertin, D. Gigmes and B. Charleux, *Prog. Polym. Sci.*, 2013, **38**, 63-235.
10. R. Poli, *Angew. Chem. Int. Ed.*, 2006, **45**, 5058-5070.
11. L. E. N. Allan, M. R. Perry and M. P. Shaver, *Prog. Polym. Sci.*, 2012, **37**, 127-156.
12. M. Kamigaito, T. Ando and M. Sawamoto, *Chem. Rev.*, 2001, **101**, 3689-3746.
13. K. Matyjaszewski and J. Xia, *Chem. Rev.*, 2001, **101**, 2921-2990.
14. J.-S. Wang and K. Matyjaszewski, *J. Am. Chem. Soc.*, 1995, **117**, 5614-5615.
15. K. Matyjaszewski, *Macromolecules*, 2012, **45**, 4015-4039.
16. K. Matyjaszewski and N. V. Tsarevsky, *J. Am. Chem. Soc.*, 2014, **136**, 6513-6533.
17. F. di Lena and K. Matyjaszewski, *Prog. Polym. Sci.*, 2010, **35**, 959-1021.
18. M. Ouchi and M. Sawamoto, *Macromolecules*, 2017, **50**, 2603-2614.
19. N. V. Tsarevsky and K. Matyjaszewski, *Chem. Rev.*, 2007, **107**, 2270-2299.
20. T. Pintauer and K. Matyjaszewski, *Chem. Soc. Rev.*, 2008, **37**, 1087-1097.
21. A. Goto, H. Zushi, N. Hirai, T. Wakada, Y. Tsujii and T. Fukuda, *J. Am. Chem. Soc.*, 2007, **129**, 13347-13354.
22. A. Goto, A. Ohtsuki, H. Ohfuji, M. Tanishima and H. Kaji, *J. Am. Chem. Soc.*, 2013, **135**, 11131-11139.
23. J. Chiefari, Y. K. Chong, F. Ercole, J. Krstina, J. Jeffery, T. P. T. Le, R. T. A. Mayadunne, G. F. Meijs, C. L. Moad, G. Moad, E. Rizzardo and S. H. Thang, *Macromolecules*, 1998, **31**, 5559-5562.
24. K. Matyjaszewski, S. Gaynor and J.-S. Wang, *Macromolecules*, 1995, **28**, 2093-2095.
25. S. Perrier, *Macromolecules*, 2017, **50**, 7433-7447.
26. A. Gregory and M. H. Stenzel, *Prog. Polym. Sci.*, 2012, **37**, 38-105.
27. H. Fischer, *Chem. Rev.*, 2001, **101**, 3581-3610.
28. W. Tang, T. Fukuda and K. Matyjaszewski, *Macromolecules*, 2006, **39**, 4332-4337.
29. W. Tang, Y. Kwak, W. Braunecker, N. V. Tsarevsky, M. L. Coote and K. Matyjaszewski, *J. Am. Chem. Soc.*, 2008, **130**, 10702-10713.
30. W. Jakubowski and K. Matyjaszewski, *Angew. Chem. Int. Ed.*, 2006, **45**, 4482-4486.
31. K. Matyjaszewski, W. Jakubowski, K. Min, W. Tang, J. Huang, W. A. Braunecker and N. V. Tsarevsky, *Proc. Natl. Acad. Sci. U.S.A.*, 2006, **103**, 15309-15314.

32. C. M. R. Abreu, P. V. Mendonça, A. n. C. Serra, A. V. Popov, K. Matyjaszewski, T. Guliashvili and J. F. J. Coelho, *ACS Macro Lett.*, 2012, **1**, 1308-1311.
33. D. Konkolewicz, Y. Wang, M. Zhong, P. Krys, A. A. Isse, A. Gennaro and K. Matyjaszewski, *Macromolecules*, 2013, **46**, 8749–8772.
34. T. Guliashvili, P. V. Mendonça, A. C. Serra, A. V. Popov and J. F. J. Coelho, *Chem. Eur. J.*, 2012, **18**, 4607-4612.
35. M. Zhong, Y. Wang, P. Krys, D. Konkolewicz and K. Matyjaszewski, *Macromolecules* 2013, **46**, 3816-3827.
36. Y. Wang, M. Zhong, W. Zhu, C.-H. Peng, Y. Zhang, D. Konkolewicz, N. Bortolamei, A. A. Isse, A. Gennaro and K. Matyjaszewski, *Macromolecules*, 2013, **46**, 3793-3802.
37. C.-H. Peng, M. Zhong, Y. Wang, Y. Kwak, Y. Zhang, W. Zhu, M. Tonge, J. Buback, S. Park, P. Krys, D. Konkolewicz, A. Gennaro and K. Matyjaszewski, *Macromolecules*, 2013, **46**, 3803-3815.
38. D. Konkolewicz, P. Krys, J. R. Góis, P. V. Mendonça, M. Zhong, Y. Wang, A. Gennaro, A. A. Isse, M. Fantin and K. Matyjaszewski, *Macromolecules*, 2014, **47**, 560-570.
39. D. Konkolewicz, Y. Wang, P. Krys, M. Zhong, A. A. Isse, A. Gennaro and K. Matyjaszewski, *Polym. Chem.*, 2014, **5**, 4396-4417.
40. Y. Zhang, Y. Wang and K. Matyjaszewski, *Macromolecules* 2011, **44**, 683-685.
41. B. M. Rosen and V. Percec, *Chem. Rev.*, 2009, **109**, 5069-5119.
42. V. Percec, T. Guliashvili, J. S. Ladislaw, A. Wistrand, A. Stjerndahl, M. J. Sienkowska, M. J. Monteiro and S. Sahoo, *J. Am. Chem. Soc.*, 2006, **128**, 14156-14165.
43. A. Anastasaki, V. Nikolaou, G. Nurumbetov, P. Wilson, K. Kempe, J. F. Quinn, T. P. Davis, M. R. Whittaker and D. M. Haddleton, *Chem. Rev.*, 2016, **116**, 835-877.
44. A. J. Teator, D. N. Lastovickova and C. W. Bielawski, *Chem. Rev.*, 2016, **116**, 1969-1992.
45. F. A. Leibfarth, K. M. Mattson, B. P. Fors, H. A. Collins and C. J. Hawker, *Angew. Chem. Int. Ed.*, 2013, **52**, 199-210.
46. A. J. D. Magenau, N. C. Strandwitz, A. Gennaro and K. Matyjaszewski, *Science*, 2011, **332**, 81-84.
47. S. Park, P. Chmielarz, A. Gennaro and K. Matyjaszewski, *Angew. Chem. Int. Ed.*, 2015, **54**, 2388-2392.
48. N. Bortolamei, A. A. Isse, A. J. D. Magenau, A. Gennaro and K. Matyjaszewski, *Angew. Chem. Int. Ed.*, 2011, **50**, 11391-11394.
49. P. Chmielarz, M. Fantin, S. Park, A. A. Isse, A. Gennaro, A. J. D. Magenau, A. Sobkowiak and K. Matyjaszewski, *Prog. Polym. Sci.*, 2017, **69**, 47-78.
50. S. Dadashi-Silab, S. Doran and Y. Yagci, *Chem. Rev.*, 2016, **116**, 10212-10275.
51. M. Chen, M. Zhong and J. A. Johnson, *Chem. Rev.*, 2016, **116**, 10167-10211.
52. X. Pan, M. A. Tasdelen, J. Laun, T. Junkers, Y. Yagci and K. Matyjaszewski, *Prog. Polym. Sci.*, 2016, **62**, 73-125.
53. H. Mohapatra, M. Kleiman and A. P. Esser-Kahn, *Nat. Chem.*, 2017, **9**, 135-139.
54. Z. Wang, X. Pan, L. Li, M. Fantin, J. Yan, Z. Wang, Z. Wang, H. Xia and K. Matyjaszewski, *Macromolecules*, 2017, **50**, 7940-7948.
55. Z. Wang, X. Pan, J. Yan, S. Dadashi-Silab, G. Xie, J. Zhang, Z. Wang, H. Xia and K. Matyjaszewski, *ACS Macro Lett.*, 2017, **6**, 546-549.

56. Z. Wang, Z. Wang, X. Pan, L. Fu, S. Lathwal, M. Olszewski, J. Yan, A. E. Enciso, Z. Wang, H. Xia and K. Matyjaszewski, *ACS Macro Lett.*, 2018, **7**, 275-280.
57. F. Lorandi, M. Fantin, A. A. Isse and A. Gennaro, *Curr. Opin. Electrochemistry*, 2018, **8**, 1-7.
58. A. J. D. Magenau, N. Bortolamei, E. Frick, S. Park, A. Gennaro and K. Matyjaszewski, *Macromolecules*, 2013, **46**, 4346-4353.
59. M. Fantin, F. Lorandi, A. Gennaro, A. A. Isse and K. Matyjaszewski, *Synthesis*, 2017, **49**, 3311-3322.
60. P. Krys and K. Matyjaszewski, *Eur. Polym. J.*, 2017, **89**, 482-523.
61. Y. Wang, M. Zhong, Y. Zhang, A. J. D. Magenau and K. Matyjaszewski, *Macromolecules*, 2012, **45**, 8929-8932.
62. M. Fantin, A. A. Isse, A. Venzo, A. Gennaro and K. Matyjaszewski, *J. Am. Chem. Soc.*, 2016, **138**, 7216-7219.
63. M. Fantin, P. Chmielarz, Y. Wang, F. Lorandi, A. A. Isse, A. Gennaro and K. Matyjaszewski, *Macromolecules*, 2017, **50**, 3726-3732.
64. M. Fantin, A. A. Isse, A. Gennaro and K. Matyjaszewski, *Macromolecules*, 2015, **48**, 6862-6875.
65. F. De Bon, M. Fantin, A. A. Isse and A. Gennaro, *Polym. Chem.*, 2018, **9**, 646-655.
66. J.-K. Guo, Y.-N. Zhou and Z.-H. Luo, *AIChE J.*, 2015, **61**, 4347-4357.
67. J.-K. Guo, Y.-N. Zhou and Z.-H. Luo, *Macromolecules*, 2016, **49**, 4038-4046.
68. J.-K. Guo, Y.-N. Zhou and Z.-H. Luo, *AIChE J.*, 2018, **64**, 961-969.
69. M. Fantin, F. Lorandi, A. A. Isse and A. Gennaro, *Macromol. Rapid Commun.*, 2016, **37**, 1318-1322.
70. C.-H. Peng, J. Kong, F. Seeliger and K. Matyjaszewski, *Macromolecules*, 2011, **44**, 7546-7557.
71. N. V. Tsarevsky, T. Sarbu, B. Göbelt and K. Matyjaszewski, *Macromolecules*, 2002, **35**, 6142-6148.
72. A. Ramakrishnan and R. Dhamodharan, *Macromolecules*, 2003, **36**, 1039-1046.
73. S. Qin, J. Saget, J. Pyun, S. Jia and T. Kowalewski, *Macromolecules*, 2003, **36**, 8969-8977.
74. B. Dufour, C. Tang, K. Koynov, Y. Zhang, T. Pakula and K. Matyjaszewski, *Macromolecules*, 2008, **41**, 2451-2458.
75. B. Dufour, K. Koynov, T. Pakula and K. Matyjaszewski, *Macromol. Chem. Phys.*, 2008, **209**, 1686-1693.
76. D. J. Siegwart, W. Wu, M. Mandalaywala, M. Tamir, T. Sarbu, M. S. Silverstein, T. Kowalewski, J. O. Hollinger and K. Matyjaszewski, *Polymer*, 2007, **48**, 7279-7290.
77. N. Kadayıfçıoğlu and H. Y. Acar, *Eur. Polym. J.*, 2013, **49**, 3366-3376.
78. S. Höhne and P. Uhlmann, *J. Polym. Sci. A: Polym. Chem.*, 2015, **53**, 675-684.
79. A. Simula, A. Anastasaki and D. M. Haddleton, *Macromol. Rapid Commun.*, 2016, **37**, 356-361.
80. L. Wu, U. Glebe and A. Böker, *Macromolecules*, 2016, **49**, 9586-9596.
81. T. J. Aitchison, M. Ginic-Markovic, S. Clarke and S. Valiyaveettil, *Macromol. Chem. Phys.*, 2012, **213**, 79-86.
82. F. Lorandi, F. De Bon, M. Fantin, A. A. Isse and A. Gennaro, *Electrochem. Commun.*, 2017, **77**, 116-119.

83. N. Bortolamei, A. A. Isse, V. B. Di Marco, A. Gennaro and K. Matyjaszewski, *Macromolecules*, 2010, **43**, 9257-9267.
84. F. Lorandi, M. Fantin, A. A. Isse and A. Gennaro, *Polym. Chem.*, 2016, **7**, 5357-5365.
85. P. Chmielarz, *Polymer*, 2016, **102**, 192-198.
86. P. Chmielarz, *Express Polym. Lett.*, 2016, **10**, 810-821.
87. P. Chmielarz, *Express Polym. Lett.*, 2017, **11**, 140-151.
88. P. Chmielarz, *Chem. Pap.*, 2017, **71**, 161-170.
89. P. Chmielarz, T. Paczesniak, K. Rydel-Ciszek, I. Zaborniak, P. Biedka and A. Sobkowiak, *Beilstein J. Org. Chem*., 2017, **13**, 2466-2472.
90. P. Chmielarz, S. Park, A. Sobkowiak and K. Matyjaszewski, *Polymer*, 2016, **88**, 36-42.
91. P. Chmielarz, A. Sobkowiak and K. Matyjaszewski, *Polymer*, 2015, **77**, 266-271.
92. N. Jasinski, A. Lauer, P. J. M. Stals, S. Behrens, S. Essig, A. Walther, A. S. Goldmann and C. Barner-Kowollik, *ACS Macro Lett.*, 2015, **4**, 298-301.
93. Y. Wei, Q. Zhang, W. J. Wang, B. G. Li and S. Zhu, *Polymer*, 2016, **106**, 261-266.
94. M. Fantin, S. Park, Y. Wang and K. Matyjaszewski, *Macromolecules*, 2016, **49**, 8838-8847.
95. Y. Wang, F. Lorandi, M. Fantin, P. Chmielarz, A. A. Isse, A. Gennaro and K. Matyjaszewski, *Macromolecules*, 2017, **50**, 8417-8425.
96. M. Fantin, A. A. Isse, K. Matyjaszewski and A. Gennaro, *Macromolecules*, 2017, **50**, 2696-2705.
97. M. Fantin, A. A. Isse, N. Bortolamei, K. Matyjaszewski and A. Gennaro, *Electrochim. Acta*, 2016, **222**, 393-401.
98. P. Chmielarz, S. Park, A. Simakova and K. Matyjaszewski, *Polymer*, 2015, **60**, 302-307.
99. L. Fu, A. Simakova, M. Fantin, Y. Wang and K. Matyjaszewski, *ACS Macro Lett.*, 2018, **7**, 26-30.
100. N. A. C. dos Santos, F. Lorandi, E. Badetti, K. Wurst, A. A. Isse, A. Gennaro, G. Licini and C. Zonta, *Polymer*, 2017, **128**, 169-176.
101. P. Chmielarz and A. Sobkowiak, *J. of Polym. Res.*, 2017, **24**, 77.
102. P. Chmielarz, P. Krys, S. Park and K. Matyjaszewski, *Polymer*, 2015, **71**, 143-147.
103. P. Chmielarz and P. Krol, in *Polyurethane Polymers: Blends and Interpenetrating Polymer Networks*, eds. S. Thomas, J. Datta, J. T. Haponiuk and A. Reghunadhan, 2017, DOI: 10.1016/b978-0-12-804039-3.00010-5, pp. 247-260.
104. P. Chmielarz and A. Sobkowiak, *Chem. Pap.*, 2016, **70**, 1228-1237.
105. P. Chmielarz, *Polym. Adv. Technol.*, 2017, **28**, 1787-1793.
106. P. Chmielarz, *Polym. Adv. Technol.* 2017, **28**, 1804-1812.
107. P. Chmielarz, *Polimery*, 2017, **62**, 642-649.
108. S. Park, H. Y. Cho, K. B. Wegner, J. Burdynska, A. J. D. Magenau, H.-j. Paik, S. Jurga and K. Matyjaszewski, *Macromolecules*, 2013, **46**, 5856-5860.
109. B. Li, B. Yu, W. T. S. Huck, W. Liu and F. Zhou, *J. Am. Chem. Soc.*, 2013, **135**, 1708-1710.
110. Y. Sun, H. Du, Y. Lan, W. Wang, Y. Liang, C. Feng and M. Yang, *Biosens. Bioelectron.*, 2016, **77**, 894-900.
111. Q. Hu, Q. Wang, G. Sun, J. Kong and X. Zhang, *Anal. Chem.*, 2017, **89**, 9253-9259.
112. S. Hosseiny and P. van Rijn, *Polymers*, 2013, **5**, 1229-1240.
113. Y. Sun, H. Du, Y. Deng, Y. Lan and C. Feng, *J. Solid State Electr.*, 2016, **20**, 105-113.

114. Y. Hu, G. Yang, B. Liang, L. Fang, G. Ma, Q. Zhu, S. Chen and X. Ye, *Acta Biomater.*, 2015, **13**, 142-149.
115. G.-P. Jin, Y. Fu, X.-C. Bao, X.-S. Feng, Y. Wang and W.-H. Liu, *J. Appl. Electrochem.*, 2014, **44**, 621-629.
116. G.-P. Jin, S.-Y. Xu, P. Lei, Y. Fu, X. Feng, Z.-X. Wu, M. Yu, S. Dai and G. Liu, *Electrochim. Acta*, 2014, **130**, 526-531.
117. L. T. Strover, J. Malmstroem, L. A. Stubbing, M. A. Brimble and J. Travas-Sejdic, *Electrochim. Acta*, 2016, **188**, 57-70.
118. J. Zhang, X.-B. Yi, W. Ju, H.-L. Fan, Q.-C. Wang, B.-X. Liu and S. Liu, *Electrochem. Commun.*, 2017, **74**, 19-23.
119. Y. Sun, J. Zhang, J. Li, M. Zhao and Y. Liu, *RSC Adv.*, 2017, **7**, 28461-28468.
120. Y. Hu, B. Liang, L. Fang, G. Ma, G. Yang, Q. Zhu, S. Chen and X. Ye, *Langmuir*, 2016, **32**, 11763-11770.
121. B. Li, B. Yu and F. Zhou, *Macromol. Rapid Commun.*, 2013, **34**, 246-250.
122. D. Chen and W. Hu, *Anal. Chem.*, 2017, **89**, 4355-4358.
123. P. Chmielarz, P. Krys, Z. Wang, Y. Wang and K. Matyjaszewski, *Macromol. Chem. Phys.*, 2017, **218**, 1700106.
124. P. Chmielarz, J. Yan, P. Krys, Y. Wang, Z. Wang, M. R. Bockstaller and K. Matyjaszewski, *Macromolecules*, 2017, **50**, 4151-4159.
125. F. Ran, D. Li and J. Wu, *Ini. J. Polym. Sci.*, 2016, DOI: 10.1155/2016/3083716.
126. J. Wu, H. Song, D. Li, W. Zhao, W. Zhang, L. Kang, F. Ran and C. Zhao, *Surfaces and Interfaces*, 2017, **8**, 119-126.
127. N. Shida, Y. Koizumi, H. Nishiyama, I. Tomita and S. Inagi, *Angew. Chem. Int. Ed.*, 2015, **54**, 3922-3926.
128. S. E. Fosdick, K. N. Knust, K. Scida and R. M. Crooks, *Angew. Chem. Int. Ed.*, 2013, **52**, 10438-10456.
129. S. Lanzalaco, M. Fantin, O. Scialdone, A. Galia, A. A. Isse, A. Gennaro and K. Matyjaszewski, *Macromolecules*, 2017, **50**, 192-202.
130. Y. Wang, M. Fantin, S. Park, E. Gottlieb, L. Fu and K. Matyjaszewski, *Macromolecules*, 2017, **50**, 7872-7879.
131. M. Falsig and H. Lund, *Acta Chem. Scand. B*, 1980, **34**, 585-590.
132. M. Falsig and H. Lund, *Acta Chem. Scand. B*, 1980, **34**, 545-549.
133. M. Falsig, H. Lund, L. Nadjo and J. M. Savéant, *Acta Chem. Scand. B*, 1980, **34**, 685-691.
134. M. A. Tasdelen, M. Uygun and Y. Yagci, *Macromol. Chem. Phys.*, 2011, **212**, 2036-2042.
135. S. Dadashi-Silab, M. A. Tasdelen, B. Kiskan, X. Wang, M. Antonietti and Y. Yagci, *Macromol. Chem. Phys.*, 2014, **215**, 675-681.
136. M. A. Tasdelen, M. Ciftci and Y. Yagci, *Macromol. Chem. Phys.*, 2012, **213**, 1391-1396.
137. M. Ciftci, M. A. Tasdelen, W. Li, K. Matyjaszewski and Y. Yagci, *Macromolecules*, 2013, **46**, 9537-9543.
138. O. S. Taskin, G. Yilmaz, M. A. Tasdelen and Y. Yagci, *Polym. Int.*, 2014, **63**, 902-907.
139. B. Li, B. Yu and F. Zhou, *Macromol. Rapid Commun.*, 2014, **35**, 1287-1292.

140. S. Dadashi-Silab, M. A. Tasdelen, A. M. Asiri, S. B. Khan and Y. Yagci, *Macromol. Rapid Commun.*, 2014, **35**, 454-459.
141. A. Bansal, A. Kumar, P. Kumar, S. Bojja, A. K. Chatterjee, S. S. Ray and S. L. Jain, *RSC Adv.*, 2015, **5**, 21189-21196.
142. Y. Cao, Y. Xu, J. Zhang, D. Yang and J. Liu, *Polymer*, 2015, **61**, 198-203.
143. J. Yan, B. Li, F. Zhou and W. Liu, *ACS Macro Lett.*, 2013, **2**, 592-596.
144. M. Ciftci, M. A. Tasdelen and Y. Yagci, *Polym. Chem.*, 2014, **5**, 600-606.
145. Y. Yagci, M. A. Tasdelen and S. Jockusch, *Polymer*, 2014, **55**, 3468-3474.
146. J.-S. Wang and K. Matyjaszewski, *Macromolecules*, 1995, **28**, 7572-7573.
147. J. Gromada and K. Matyjaszewski, *Macromolecules*, 2001, **34**, 7664-7671.
148. Z. Guan and B. Smart, *Macromolecules*, 2000, **33**, 6904-6906.
149. Y. Kwak and K. Matyjaszewski, *Macromolecules*, 2010, **43**, 5180-5183.
150. M. A. Tasdelen, M. Uygun and Y. Yagci, *Macromol. Chem. Phys.*, 2010, **211**, 2271-2275.
151. M. A. Tasdelen, M. Uygun and Y. Yagci, *Macromol. Rapid Commun.*, 2011, **32**, 58-62.
152. J. Mosnáček and M. Ilčíková, *Macromolecules*, 2012, **45**, 5859-5865.
153. D. Konkolewicz, K. Schroder, J. Buback, S. Bernhard and K. Matyjaszewski, *ACS Macro Lett.*, 2012, **1**, 1219-1223.
154. A. Anastasaki, V. Nikolaou, Q. Zhang, J. Burns, S. R. Samanta, C. Waldron, A. J. Haddleton, R. McHale, D. Fox, V. Percec, P. Wilson and D. M. Haddleton, *J. Am. Chem. Soc.*, 2014, **136**, 1141-1149.
155. T. G. Ribelli, D. Konkolewicz, S. Bernhard and K. Matyjaszewski, *J. Am. Chem. Soc.*, 2014, **136**, 13303-13312.
156. J. Mosnáček, A. Eckstein-Andicsová and K. Borská, *Polym. Chem.*, 2015, **6**, 2523-2530.
157. G.-X. Wang, M. Lu, Z.-H. Hou, C.-A. Yang, E.-X. Liang, L.-c. Liu, H. Wu, X.-L. Li and Y.-X. Xu, *J. Polym. Res.*, 2015, **22**, 60.
158. T. Zhang, T. Chen, I. Amin and R. Jordan, *Polym. Chem.*, 2014, **5**, 4790-4796.
159. A. Anastasaki, V. Nikolaou, N. W. McCaul, A. Simula, J. Godfrey, C. Waldron, P. Wilson, K. Kempe and D. M. Haddleton, *Macromolecules*, 2015, **48**, 1404-1411.
160. W. Tang and K. Matyjaszewski, *Macromolecules*, 2007, **40**, 1858-1863.
161. J. Mosnacek, A. Kundys and A. Andicsova, *Polymers*, 2014, **6**, 2862-2874.
162. E. Larsson, S. A. Pendergraph, T. Kaldeus, E. Malmstrom and A. Carlmark, *Polym. Chem.*, 2015, **6**, 1865-1874.
163. A. Anastasaki, V. Nikolaou, G. Nurumbetov, N. P. Truong, G. S. Pappas, N. G. Engelis, J. F. Quinn, M. R. Whittaker, T. P. Davis and D. M. Haddleton, *Macromolecules*, 2015, **48**, 5140-5147.
164. A. Anastasaki, V. Nikolaou, A. Simula, J. Godfrey, M. Li, G. Nurumbetov, P. Wilson and D. M. Haddleton, *Macromolecules*, 2014, **47**, 3852-3859.
165. A. Anastasaki, V. Nikolaou, G. S. Pappas, Q. Zhang, C. Wan, P. Wilson, T. P. Davis, M. R. Whittaker and D. M. Haddleton, *Chem. Sci.*, 2014, **5**, 3536-3542.
166. A. Anastasaki, V. Nikolaou, F. Brandford-Adams, G. Nurumbetov, Q. Zhang, G. J. Clarkson, D. J. Fox, P. Wilson, K. Kempe and D. M. Haddleton, *Chem. Commun.*, 2015, **51**, 5626-5629.

167. V. Nikolaou, A. Anastasaki, F. Alsubaie, A. Simula, D. J. Fox and D. M. Haddleton, *Polym. Chem.*, 2015, **6**, 3581-3585.
168. H.-C. Lee, M. Fantin, M. Antonietti, K. Matyjaszewski and B. V. K. J. Schmidt, *Chem. Mater.*, 2017, **29**, 9445-9455.
169. Q. Yang, F. Dumur, F. Morlet-Savary, J. Poly and J. Lalevée, *Macromolecules*, 2015, **48**, 1972-1980.
170. Q. Yang, J. Lalevée and J. Poly, *Macromolecules*, 2016, **49**, 7653-7666.
171. Y.-M. Chuang, A. Ethirajan and T. Junkers, *ACS Macro Lett.*, 2014, **3**, 732.
172. Y. M. Chuang, B. Wenn, S. Gielen, A. Ethirajan and T. Junkers, *Polym. Chem.*, 2015, **6**, 6488-6497.
173. B. Wenn, M. Conradi, A. D. Carreiras, D. M. Haddleton and T. Junkers, *Polym. Chem.*, 2014, **5**, 3053-3060.
174. S. Chantasirichot, Y. Inoue and K. Ishihara, *Polymer*, 2015, **61**, 55-60.
175. E. H. Discekici, A. Anastasaki, R. Kaminker, J. Willenbacher, N. P. Truong, C. Fleischmann, B. Oschmann, D. J. Lunn, J. Read de Alaniz, T. P. Davis, C. M. Bates and C. J. Hawker, *J. Am. Chem. Soc.*, 2017, **139**, 5939-5945.
176. X. Pan, N. Malhotra, A. Simakova, Z. Wang, D. Konkolewicz and K. Matyjaszewski, *J. Am. Chem. Soc.*, 2015, **137**, 15430-15433.
177. G. R. Jones, R. Whitfield, A. Anastasaki and D. M. Haddleton, *J. Am. Chem. Soc.*, 2016, **138**, 7346-7352.
178. E. Frick, A. Anastasaki, D. M. Haddleton and C. Barner-Kowollik, *J. Am. Chem. Soc.*, 2015, **137**, 6889-6896.
179. T. G. Ribelli, D. Konkolewicz, X. Pan and K. Matyjaszewski, *Macromolecules*, 2014, **47**, 6316-6321.
180. T. Zhang, D. Gieseler and R. Jordan, *Polym. Chem.*, 2016, **7**, 775-779.
181. Z. Xue, D. He and X. Xie, *Polym. Chem.*, 2015, **6**, 1660-1687.
182. R. Poli, L. E. N. Allan and M. P. Shaver, *Prog. Polym. Sci.*, 2014, **39**, 1827-1845.
183. Z. Xue, N. T. B. Linh, S. K. Noh and W. S. Lyoo, *Angew. Chem. Int. Ed.*, 2008, **47**, 6426-6429.
184. Y. Wang, Y. Kwak and K. Matyjaszewski, *Macromolecules*, 2012, **45**, 5911-5915.
185. T. Ando, M. Kamigaito and M. Sawamoto, *Macromolecules*, 1997, **30**, 4507-4510.
186. K. Matyjaszewski, M. Wei, J. Xia and N. E. McDermott, *Macromolecules*, 1997, **30**, 8161-8164.
187. A. Simakova, M. Mackenzie, S. E. Averick, S. Park and K. Matyjaszewski, *Angew. Chem. Int. Ed.*, 2013, **52**, 12148-12151.
188. Y. Wang and K. Matyjaszewski, *Macromolecules*, 2010, **43**, 4003-4005.
189. Q.-L. Zhao, E.-H. Liu, G.-X. Wang, Z.-H. Hou, X.-H. Zhan, L.-c. Liu and H. Wu, *J. Polym. Res.*, 2014, **21**, 1-6.
190. G.-X. Wang, M. Lu, Z.-H. Hou, Y. Gao, L.-C. Liu and H. Wu, *J. Macromol. Sci. A*, 2014, **51**, 565-571.
191. L.-c. Liu, M. Lu, Z.-H. Hou, G.-X. Wang, C.-A. Yang, E.-X. Liang, H. Wu, X.-L. Li and Y.-X. Xu, *J. Appl. Polym. Sci.*, 2015, **132**, 42389.
192. A. Bansal, P. Kumar, C. D. Sharma, S. S. Ray and S. L. Jain, *J. Polym. Sci. A: Polym. Chem.*, 2015, **53**, 2739-2746.

193. S. Telitel, F. Dumur, D. Campolo, J. Poly, D. Gigmes, J. Pierre Fouassier and J. Lalevée, *J. Polym. Sci. A: Polym. Chem.*, 2016, **54**, 702-713.
194. X. Pan, N. Malhotra, J. Zhang and K. Matyjaszewski, *Macromolecules*, 2015, **48**, 6948-6954.
195. X. Pan, N. Malhotra, S. Dadashi-Silab and K. Matyjaszewski, *Macromol. Rapid Commun.*, 2017, **38**, 1600651.
196. Y.-N. Zhou, J.-K. Guo, J.-J. Li and Z.-H. Luo, *Ind. Eng. Chem. Res.*, 2016, **55**, 10235-10242.
197. C. Bian, Y.-N. Zhou, J.-K. Guo and Z.-H. Luo, *Ind. Eng. Chem. Res.*, 2017, **56**, 4949-4956.
198. S. Dadashi-Silab, X. Pan and K. Matyjaszewski, *Macromolecules*, 2017, **50**, 7967-7977.
199. C. Bian, Y.-N. Zhou, J.-K. Guo and Z.-H. Luo, *Polym. Chem.*, 2017, **8**, 7360-7368.
200. K. Iwai, M. Uesugi and F. Takemura, *Polym. J.*, 1985, **17**, 1005-1011.
201. G. Zhang, I. Y. Song, K. H. Ahn, T. Park and W. Choi, *Macromolecules*, 2011, **44**, 7594-7599.
202. N. V. Alfredo, N. E. Jalapa, S. L. Morales, A. D. Ryabov, R. Le Lagadec and L. Alexandrova, *Macromolecules*, 2012, **45**, 8135-8146.
203. F. Nzulu, S. Telitel, F. Stoffelbach, B. Graff, F. Morlet-Savary, J. Lalevee, L. Fensterbank, J.-P. Goddard and C. Ollivier, *Polym. Chem.*, 2015, **6**, 4605-4611.
204. C. K. Prier, D. A. Rankic and D. W. C. MacMillan, *Chem. Rev.*, 2013, **113**, 5322-5363.
205. D. A. Nicewicz and D. W. C. MacMillan, *Science*, 2008, **322**, 77-80.
206. C.-J. Wallentin, J. D. Nguyen, P. Finkbeiner and C. R. J. Stephenson, *J. Am. Chem. Soc.*, 2012, **134**, 8875-8884.
207. J. D. Nguyen, J. W. Tucker, M. D. Konieczynska and C. R. J. Stephenson, *J. Am. Chem. Soc.*, 2011, **133**, 4160-4163.
208. B. P. Fors and C. J. Hawker, *Angew. Chem. Int. Ed.*, 2012, **51**, 8850-8853.
209. W. Ma, H. Chen, Y. Ma, C. Zhao and W. Yang, *Macromol. Chem. Phys.*, 2014, **215**, 1012-1021.
210. Q. Liu, L. Liu, Y. Ma, C. Zhao and W. Yang, *J. Polym. Sci. A: Polym. Chem.*, 2014, **52**, 3283-3291.
211. W. Ma, D. Chen, L. Wang, Y. Ma, C. Zhao and W. Yang, *J. Macromol. Sci. A*, 2015, **52**, 761-769.
212. N. J. Treat, B. P. Fors, J. W. Kramer, M. Christianson, C.-Y. Chiu, J. R. d. Alaniz and C. J. Hawker, *ACS Macro Lett.*, 2014, **3**, 580-584.
213. X. Liu, Y. Ni, J. Wu, H. Jiang, Z. Zhang, L. Zhang, Z. Cheng and X. Zhu, *Polym. Chem.*, 2018, **9**, 584-592.
214. S. Telitel, F. Dumur, S. Telitel, O. Soppera, M. Lepeltier, Y. Guillaneuf, J. Poly, F. Morlet-Savary, P. Fioux, J.-P. Fouassier, D. Gigmes and J. Lalevée, *Polym. Chem.*, 2015, **6**, 613-624.
215. J. Kreutzer and Y. Yagci, *Polymers-Basel*, 2018, **10**, 35.
216. J. C. Theriot, B. G. McCarthy, C.-H. Lim and G. M. Miyake, *Macromol. Rapid Commun.*, 2017, **38**, 1700040.
217. N. J. Treat, H. Sprafke, J. W. Kramer, P. G. Clark, B. E. Barton, J. Read de Alaniz, B. P. Fors and C. J. Hawker, *J. Am. Chem. Soc.*, 2014, **136**, 16096-16101.
218. X. Pan, C. Fang, M. Fantin, N. Malhotra, W. Y. So, L. A. Peteanu, A. A. Isse, A. Gennaro, P. Liu and K. Matyjaszewski, *J. Am. Chem. Soc.*, 2016, **138**, 2411-2425.
219. S. Dadashi-Silab, X. Pan and K. Matyjaszewski, *Chem. Eur. J.*, 2017, **23**, 5972-5977.
220. S. Li, A. I. Mohamed, V. Pande, H. Wang, J. Cuthbert, X. Pan, H. He, Z. Wang, V. Viswanathan, J. F. Whitacre and K. Matyjaszewski, *ACS Energy Lett.*, 2018, **3**, 20-27.

221. J. Wang, L. Yuan, Z. Wang, M. A. Rahman, Y. Huang, T. Zhu, R. Wang, J. Cheng, C. Wang, F. Chu and C. Tang, *Macromolecules*, 2016, **49**, 7709-7717.

222. X. Pan, M. Lamson, J. Yan and K. Matyjaszewski, *ACS Macro Lett.*, 2015, **4**, 192-196.

223. K. Matyjaszewski, S. M. Jo, H.-j. Paik and D. A. Shipp, *Macromolecules*, 1999, **32**, 6431-6438.

224. K. Matyjaszewski, S. Mu Jo, H.-j. Paik and S. G. Gaynor, *Macromolecules*, 1997, **30**, 6398-6400.

225. T. Kowalewski, N. V. Tsarevsky and K. Matyjaszewski, *J. Am. Chem. Soc.*, 2002, **124**, 10632-10633.

226. J. P. McGann, M. Zhong, E. K. Kim, S. Natesakhawat, M. Jaroniec, J. F. Whitacre, K. Matyjaszewski and T. Kowalewski, *Macromol. Chem. Phys.*, 2012, **213**, 1078-1090.

227. M. Zhong, S. Natesakhawat, J. P. Baltrus, D. Luebke, H. Nulwala, K. Matyjaszewski and T. Kowalewski, *Chem. Commun.*, 2012, **48**, 11516-11518.

228. M. Zhong, E. K. Kim, J. P. McGann, S.-E. Chun, J. F. Whitacre, M. Jaroniec, K. Matyjaszewski and T. Kowalewski, *J. Am. Chem. Soc.*, 2012, **134**, 14846-14857.

229. S. Jockusch and Y. Yagci, *Polym. Chem.*, 2016, **7**, 6039-6043.

230. E. H. Discekici, N. J. Treat, S. O. Poelma, K. M. Mattson, Z. M. Hudson, Y. Luo, C. J. Hawker and J. R. de Alaniz, *Chem. Commun.*, 2015, **51**, 11705-11708.

231. S. O. Poelma, G. L. Burnett, E. H. Discekici, K. M. Mattson, N. J. Treat, Y. Luo, Z. M. Hudson, S. L. Shankel, P. G. Clark, J. W. Kramer, C. J. Hawker and J. Read de Alaniz, *J. Org. Chem.*, 2016, **81**, 7155-7160.

232. R. A. Marcus, *J. Chem. Phys.*, 1956, **24**, 966-978.

233. L. Pause, M. Robert and J.-M. Savéant, *J. Am. Chem. Soc.*, 2000, **122**, 9829-9835.

234. J. M. Saveant, *J. Am. Chem. Soc.*, 1987, **109**, 6788-6795.

235. J. M. Saveant, *J. Am. Chem. Soc.*, 1992, **114**, 10595-10602.

236. J. C. Theriot, C. H. Lim, H. Yang, M. D. Ryan, C. B. Musgrave and G. M. Miyake, *Science*, 2016, **352**, 1082-1086.

237. C.-H. Lim, M. D. Ryan, B. G. McCarthy, J. C. Theriot, S. M. Sartor, N. H. Damrauer, C. B. Musgrave and G. M. Miyake, *J. Am. Chem. Soc.*, 2017, **139**, 348-355.

238. M. D. Ryan, J. C. Theriot, C.-H. Lim, H. Yang, A. G. Lockwood, N. G. Garrison, S. R. Lincoln, C. B. Musgrave and G. M. Miyake, *J. Polym. Sci. A: Polym. Chem.*, 2017, **55**, 3017-3027.

239. D. Koyama, H. J. A. Dale and A. J. Orr-Ewing, *J. Am. Chem. Soc.*, 2018, **140**, 1285-1293.

240. G. M. Miyake and J. C. Theriot, *Macromolecules*, 2014, **47**, 8255-8261.

241. C. Aydogan, G. Yilmaz and Y. Yagci, *Macromolecules*, 2017, **50**, 9115-9120.

242. A. Allushi, S. Jockusch, G. Yilmaz and Y. Yagci, *Macromolecules*, 2016, **49**, 7785-7792.

243. R. M. Pearson, C.-H. Lim, B. G. McCarthy, C. B. Musgrave and G. M. Miyake, *J. Am. Chem. Soc.*, 2016, **138**, 11399-11407.

244. M. D. Ryan, R. M. Pearson, T. A. French and G. M. Miyake, *Macromolecules*, 2017, **50**, 4616-4622.

245. B. L. Buss, L. R. Beck and G. M. Miyake, *Polym. Chem.*, 2018, **9**, 1658-1665.

246. C. Kutahya, A. Allushi, R. Isci, J. Kreutzer, T. Ozturk, G. Yilmaz and Y. Yagci, *Macromolecules*, 2017, **50**, 6903-6910.

247. Z. Huang, Y. Gu, X. Liu, L. Zhang, Z. Cheng and X. Zhu, *Macromol. Rapid Commun.*, 2017, **38**, 1600461.
248. X. D. Liu, L. F. Zhang, Z. P. Cheng and X. L. Zhu, *Polym. Chem.*, 2016, **7**, 689-700.
249. T. Niu, J. Jiang, S. Li, B. Ni, X. Liu and M. Chen, *Macromol. Chem. Phys.*, 2017, **218**, 1700169.
250. Y. Yang, X. Liu, G. Ye, S. Zhu, Z. Wang, X. Huo, K. Matyjaszewski, Y. Lu and J. Chen, *ACS Appl. Mater. Interfaces*, 2017, **9**, 13637-13646.
251. C. Kutahya, F. S. Aykac, G. Yilmaz and Y. Yagci, *Polym. Chem.*, 2016, **7**, 6094-6098.
252. A. Allushi, C. Kutahya, C. Aydogan, J. Kreutzer, G. Yilmaz and Y. Yagci, *Polym. Chem.*, 2017, **8**, 1972-1977.
253. J. Vandenbergh, G. Reekmans, P. Adriaensens and T. Junkers, *Chem. Commun.*, 2013, **49**, 10358-10360.
254. J. Vandenbergh, G. Reekmans, P. Adriaensens and T. Junkers, *Chem. Sci.*, 2015, **6**, 5753-5761.
255. T. Junkers and B. Wenn, *React. Chem. Eng.*, 2016, **1**, 60-64.
256. L. D. Elliott, J. P. Knowles, P. J. Koovits, K. G. Maskill, M. J. Ralph, G. Lejeune, L. J. Edwards, R. I. Robinson, I. R. Clemens, B. Cox, D. D. Pascoe, G. Koch, M. Eberle, M. B. Berry and K. I. Booker-Milburn, *Chem. Eur. J.* 2014, **20**, 15226-15232.
257. A. Melker, B. P. Fors, C. J. Hawker and J. E. Poelma, *J. Polym. Sci. A: Polym. Chem.*, 2015, **53**, 2693-2698.
258. B. L. Ramsey, R. M. Pearson, L. R. Beck and G. M. Miyake, *Macromolecules*, 2017, **50**, 2668-2674.
259. J. Laun, M. Vorobii, A. de Los Santos Pereira, O. Pop-Georgievski, V. Trouillet, A. Welle, C. Barner-Kowollik, C. Rodriguez-Emmenegger and T. Junkers, *Macromol. Rapid Commun.*, 2015, **36**, 1681-1686.
260. M. Vorobii, A. de los Santos Pereira, O. Pop-Georgievski, N. Y. Kostina, C. Rodriguez-Emmenegger and V. Percec, *Polym. Chem.*, 2015, **6**, 4210-4220.
261. J. E. Poelma, B. P. Fors, G. F. Meyers, J. W. Kramer and C. J. Hawker, *Angew. Chem. Int. Ed.*, 2013, **52**, 6844-6848.
262. C. W. Pester, J. E. Poelma, B. Narupai, S. N. Patel, G. M. Su, T. E. Mates, Y. Luo, C. K. Ober, C. J. Hawker and E. J. Kramer, *J. Polym. Sci. A: Polym. Chem.*, 2016, **54**, 253-262.
263. E. H. Discekici, C. W. Pester, N. J. Treat, J. Lawrence, K. M. Mattson, B. Narupai, E. P. Toumayan, Y. Luo, A. J. McGrath, P. G. Clark, J. Read de Alaniz and C. J. Hawker, *ACS Macro Lett.*, 2016, **5**, 258-262.
264. J. Yan, X. Pan, M. Schmitt, Z. Wang, M. R. Bockstaller and K. Matyjaszewski, *ACS Macro Lett.*, 2016, **5**, 661-665.
265. J. Yan, X. Pan, Z. Wang, J. Zhang and K. Matyjaszewski, *Macromolecules*, 2016, **49**, 9283-9286.
266. X. Pan, S. Lathwal, S. Mack, J. Yan, S. R. Das and K. Matyjaszewski, *Angew. Chem. Int. Ed.*, 2017, **56**, 2740-2743.
267. A. Beziau, A. Fortney, L. Fu, C. Nishiura, H. Wang, J. Cuthbert, E. Gottlieb, A. C. Balazs, T. Kowalewski and K. Matyjaszewski, *Polymer*, 2017, **126**, 224-230.
268. M. Chen, Y. Gu, A. Singh, M. Zhong, A. M. Jordan, S. Biswas, L. T. J. Korley, A. C. Balazs and J. A. Johnson, *ACS Cent. Sci.*, 2017, **3**, 124-134.

269. A. B. Julia Cuthbert, Liye Fu, Chiaki Nishiura, Tomasz Kowalewski, Krzysztof Matyjaszewski, *Macromolecules*, **in press**.
270. M. Chen, S. Deng, Y. Gu, J. Lin, M. J. MacLeod and J. A. Johnson, *J. Am. Chem. Soc.*, 2017, **139**, 2257-2266.
271. K.-S. Hong, H. Xu, H. Konishi and X. Li, *J. Phys. Chem. Lett.*, 2010, **1**, 997-1002.
272. X. Wang, J. Song, J. Liu and Z. L. Wang, *Science*, 2007, **316**, 102-105.
273. J. M. J. Paulusse and R. P. Sijbesma, *J. Polym. Sci. A: Polym. Chem.*, 2006, **44**, 5445-5453.
274. F. S. French, *Annu. Rev. Physiol.*, 1992, **54**, 135-152.
275. T. G. McKenzie, E. Colombo, Q. Fu, M. Ashokkumar and G. G. Qiao, *Angew. Chem. Int. Ed.*, 2017, **56**, 12302-12306.
276. L. Mueller, W. Jakubowski, W. Tang and K. Matyjaszewski, *Macromolecules* 2007, **40**, 6464-6472.
277. J. Pietrasik, H. Dong and K. Matyjaszewski, *Macromolecules* 2006, **39**, 6384-6390.
278. H. Dong, W. Tang and K. Matyjaszewski, *Macromolecules*, 2007, **40**, 2974-2977.
279. W. Jakubowski, K. Min and K. Matyjaszewski, *Macromolecules* 2006, **39**, 39-45.
280. K. Min, H. Gao and K. Matyjaszewski, *Macromolecules*, 2007, **40**, 1789-1791.
281. Y. Kwak, A. J. D. Magenau and K. Matyjaszewski, *Macromolecules*, 2011, **44**, 811-819.
282. K. Matyjaszewski, Hongchen Dong, W. Jakubowski, J. Pietrasik and A. Kusumo, *Langmuir* 2007, **23**, 4528-4531.
283. R. Nicolay, Y. Kwak and K. Matyjaszewski, *Angew. Chem. Int. Ed.*, 2010, **49**, 541-544.
284. Y. Kwak and K. Matyjaszewski, *Polym. Int.*, 2009, **58**, 242-247.
285. H. Dong and K. Matyjaszewski, *Macromolecules* 2008, **41**, 6868-6870.
286. G.-X. Wang, M. Lu, L.-C. Liu, H. Wu and M. Zhong, *J. Appl. Polym. Sci.*, 2013, **128**, 3077-3083.
287. X.-S. Wang and S. P. Armes, *Macromolecules*, 2000, **33**, 6640-6647.
288. A. Simakova, S. E. Averick, D. Konkolewicz and K. Matyjaszewski, *Macromolecules*, 2012, **45**, 6371-6379.
289. S. Chantasirichot, Y. Inoue and K. Ishihara, *Polymer*, 2017, **123**, 100-106.
290. H. Ding, S. Park, M. Zhong, X. Pan, J. Pietrasik, C. J. Bettinger and K. Matyjaszewski, *Macromolecules*, 2016, **49**, 6752-6760.
291. D. Xiong, N. Yao, H. Gu, J. Wang and L. Zhang, *Polymer*, 2017, **114**, 161-172.
292. N. Yao, W. Lin, X. Zhang, H. Gu and L. Zhang, *J. Polym. Sci. A: Polym. Chem.*, 2016, **54**, 186-196.
293. T. Nishimura, F. Tamura, S. Kobayashi, Y. Tanimoto, F. Hayashi, Y. Sudo, Y. Iwasaki and K. Morigaki, *Langmuir*, 2017, **33**, 5752-5759.
294. Y. Q. Yang, W. J. Lin, B. Zhao, X. F. Wen, X. D. Guo and L. J. Zhang, *Langmuir*, 2012, **28**, 8251-8259.
295. G. Ye, J. Lee, F. Perreault and M. Elimelech, *ACS Appl. Mater. Interfaces*, 2015, **7**, 23069-23079.
296. D. Hong, H. C. Hung, K. Wu, X. Lin, F. Sun, P. Zhang, S. Liu, K. E. Cook and S. Jiang, *ACS Appl. Mater. Interfaces*, 2017, **9**, 9255-9259.
297. J. Ren, D. Yu, L. Feng, G. Wang and G. Lv, *Compos. Part A Appl. Sci. Manuf.*, 2017, **98**, 66-75.
298. S. E. Averick, C. G. Bazewicz, B. F. Woodman, A. Simakova, R. A. Mehl and K. Matyjaszewski, *Eur. Polym. J.*, 2013, **49**, 2919-2924.

299. G. Yaşayan, A. O. Saeed, F. Fernández-Trillo, S. Allen, M. C. Davies, A. Jangher, A. Paul, K. J. Thurecht, S. M. King, R. Schweins, P. C. Griffiths, J. P. Magnusson and C. Alexander, *Polym. Chem.*, 2011, **2**, 1567.
300. K. Matyjaszewski and K. L. Beers, *J. Chem. Educ.* 2001, **78**, 547-550.
301. K. Matyjaszewski, S. Coca, S. G. Gaynor, M. Wei and B. E. Woodworth, *Macromolecules* 1997, **30**, 7348-7350.
302. K. Matyjaszewski, S. G. Gaynor, S. Coca. Controlled atom or group-transfer radical polymerization, coupling of molecules, multifunctional polymerization initiators, and formation of telechelic functional material. 1998, Patent no. 9840415, 19980917.
303. K. Matyjaszewski, S. Coca, S. G. Gaynor, M. Wei and B. E. Woodworth, *Macromolecules*, 1998, **31**, 5967-5969.
304. V. A. Williams, T. G. Ribelli, P. Chmielarz, S. Park and K. Matyjaszewski, *J. Am. Chem. Soc.,* 2015, **137**, 1428-1431.
305. P. Krys, T. G. Ribelli, K. Matyjaszewski and A. Gennaro, *Macromolecules*, 2016, **49**, 2467-2476.
306. P. Krys, Y. Wang, K. Matyjaszewski and S. Harrisson, *Macromolecules*, 2016, **49**, 2977-2984.
307. R. A. Cordeiro, N. Rocha, J. P. Mendes, K. Matyjaszewski, T. Guliashvili, A. n. C. Cerra and J. F. J. Coelho, *Polym. Chem.*, 2013, **4**, 3088-3097.
308. V. A. Williams and K. Matyjaszewski, *Macromolecules*, 2015, **48**, 6457-6464.
309. C. M. R. Abreu, A. e. C. Serra, A. V. Popov, K. Matyjaszewski, T. Guliashvili and J. F. J. Coelho, *Polym. Chem.* 2013, **4**, 5629-5636.
310. J. o. R. C. Costa, P. V. Mendonça, P. Maximiano, A. n. C. Serra, T. Guliashvili and J. F. J. Coelho, *Macromolecules*, 2015, **48**, 6810-6815.
311. J. P. Mendes, F. b. Branco, C. M. R. Abreu, P. V. Mendonça, A. V. Popov, T. Guliashvili, A. n. C. Serra and J. F. J. Coelho, *ACS Macro Lett.*, 2014, **3**, 544-547.
312. P. Krys, M. Fantin, P. V. Mendonca, C. M. R. Abreu, T. Guliashvili, J. Rosa, L. O. Santos, A. C. Serra, K. Matyjaszewski and J. F. J. Coelho, *Polym. Chem.*, 2017, **8**, 6506-6519.
313. P. Chmielarz and P. Król, *eXPRESS Polym. Lett.,* 2016, **10**, 302-310.
314. J. R. Góis, A. C. Serra and J. F. J. Coelho, *Eur. Polym. J.* 2016, **81**, 224-238.
315. A. Nese, Y. Li, S. S. Sheiko and K. Matyjaszewski, *ACS Macro Lett.*, 2012, **1**, 991-994.
316. J. Yan, X. Pan, Z. Wang, Z. Lu, Y. Wang, L. Liu, J. Zhang, C. Ho, M. R. Bockstaller and K. Matyjaszewski, *Chem. Mater.*, 2017, **29**, 4963-4969.
317. C. Zhou, Y. Wu, K. R. V. Thappeta, J. T. L. Subramanian, D. Pranantyo, E.-T. Kang, H. Duan, K. Kline and M. B. Chan-Park, *ACS Appl. Mater. Interfaces* 2017, **9**, 36269-36280.
318. T. Zhang, Y. Du, F. Muller, I. Amin and R. Jordan, *Polym. Chem.*, 2015, **6**, 2726-2733.
319. T. Zhang, Y. Du, J. Kalbacova, R. Schubel, R. D. Rodriguez, T. Chen, D. R. T. Zahn and R. Jordan, *Polym. Chem.*, 2015, **6**, 8176-8183.
320. E. S. Dehghani, Y. Du, T. Zhang, S. N. Ramakrishna, N. D. Spencer, R. Jordan and E. M. Benetti, *Macromolecules*, 2017, **50**, 2436-2446.
321. S. Dadashi-Silab and K. Matyjaszewski, *Macromolecules*, 2018, **Submitted**.
322. P. Krys, H. Schroeder, J. Buback, M. Buback and K. Matyjaszewski, *Macromolecules*, 2016, **49**, 7793-7803.

323. D. Konkolewicz, A. J. D. Magenau, S. E. Averick, A. Simakova, H. He and K. Matyjaszewski, *Macromolecules*, 2012, **45**, 4461-4468.
324. J. Wu, X. Jiang, L. Zhang, Z. Cheng and X. Zhu, *Polymers-Basel*, 2016, **8**, 29.
325. Z. Huang, J. Chen, L. Zhang, Z. Cheng and X. Zhu, *Polymers-Basel*, 2016, **8**, 59.
326. X.-h. Liu, J. Wang, F.-j. Zhang, S.-l. An, Y.-l. Ren, Y.-h. Yu, P. Chen and S. Xie, *J. Polym. Sci. A: Polym. Chem.*, 2012, **50**, 4358-4364.
327. N. V. Tsarevsky and W. Jakubowski, *J. Polym. Sci. A: Polym. Chem.*, 2011, **49**, 918-925.
328. Y. Wang, Y. Zhang, B. Parker and K. Matyjaszewski, *Macromolecules*, 2011, **44**, 4022-4025.
329. L. Zhang, J. Miao, Z. Cheng and X. Zhu, *Macromol. Rapid Commun.*, 2010, **31**, 275-280.
330. G. Wang, M. Lu, M. Zhong and H. Wu, *J. Polym. Res.*, 2012, **19**, 9782.
331. M. Ding, X. Jiang, J. Peng, L. Zhang, Z. Cheng and X. Zhu, *Green Chem.*, 2015, **17**, 271-278.
332. G. Wang, Z. Wang, B. Lee, R. Yuan, Z. Lu, J. Yan, X. Pan, Y. Song, M. R. Bockstaller and K. Matyjaszewski, *Polymer*, 2017, **129**, 57-67.
333. D. D'Hooge, P. Van Steenberge, M.-F. Reyniers and G. Marin, *Polymers*, 2014, **6**, 1074-1095.
334. G. Wang, M. Schmitt, Z. Wang, B. Lee, X. Pan, L. Fu, J. Yan, S. Li, G. Xie, M. R. Bockstaller and K. Matyjaszewski, *Macromolecules*, 2016, **49**, 8605-8615.
335. J. P. Sun, Y. Zhang, J. Li, C. Y. Wang and Q. Ren, *J. Nano Res.*, 2016, **41**, 63-73.
336. Y. Song, G. Ye, Z. Wang, M. Kopeć, G. Xie, R. Yuan, J. Chen, T. Kowalewski, J. Wang and K. Matyjaszewski, *Macromolecules*, 2016, **49**, 8943-8950.
337. Y. Liu, X. Liu, G. Ye, Y. Song, F. Liu, X. Huo and J. Chen, *Dalton Trans.*, 2017, **46**, 6117-6127.
338. J. Yin, Z. Wang, M. Song, C. Zhao and H. Wang, *The Analyst*, 2013, **138**, 4958-4966.
339. W. Wang, P. Julaiti, G. Ye, X. Huo, Y. Lu and J. Chen, *Ind. Eng. Chem. Res.*, 2017, **56**, 11467-11476.
340. F. Oytun, M. U. Kahveci and Y. Yagci, *J. Polym. Sci. A: Polym. Chem.*, 2013, **51**, 1685-1689.
341. R. Chapman, A. J. Gormley, K.-L. Herpoldt and M. M. Stevens, *Macromolecules*, 2014, **47**, 8541-8547.
342. R. Chapman, A. J. Gormley, M. H. Stenzel and M. M. Stevens, *Angew. Chem. Int. Ed.*, 2016, **55**, 4500-4503.
343. Z. Liu, Y. Lv and Z. An, *Angew. Chem. Int. Ed.*, 2017, **56**, 13852-13856.
344. A. E. Enciso, L. Fu, A. J. Russell and K. Matyjaszewski, *Angew. Chem. Int. Ed.*, 2018, **57**, 933-936.
345. W. Jakubowski, in *Progress in Controlled Radical Polymerization: Mechanisms and Techniques*, American Chemical Society, 2012, vol. 1100, ch. 13, pp. 203-216.
346. S. Shanmugam, J. Xu and C. Boyer, *Angew. Chem. Int. Ed.*, 2016, **55**, 1036-1040.
347. J. Xu, S. Shanmugam, C. Fu, K.-F. Aguey-Zinsou and C. Boyer, *J. Am. Chem. Soc.*, 2016, **138**, 3094-3106.
348. A. B. Biernesser, K. R. D. Chiaie, J. B. Curley and J. A. Byers, *Angew. Chem. Int. Ed.*, 2016, **55**, 5251-5254.

ToC graphics